

POLITECNICO DI TORINO

Master's Degree in Mechanical Engineering



**Politecnico
di Torino**

Master's Degree Thesis

Optimization of support structures for turbine blades with EBM process

Supervisors

Prof. Luca Iuliano

Candidate

Antonio Petitto

Luglio 2022

POLITECNICO DI TORINO

Master's Degree in Mechanical Engineering



**Politecnico
di Torino**

Master's Degree Thesis

Optimization of support structures for turbine blades with EBM process



Tutor

Ing. Carmelo Giorgio

(Avio Aero)

Candidate

Antonio Petitto

Luglio 2022

Abstract

This thesis work is based on the optimization of a particular type of support structures for the production by AM of an aircraft component. At the state of the art, the studied supports are used in the company's field for the production of low-pressure turbine blades by EBM process. EBM is a powder bed fusion process, which employs a concentrated electron beam for the production of layer-by-layer components. The purpose of this thesis is to optimize this process through the study, modification, implementation and development of the currently adopted supports for turbine blades. In particular, as will be highlighted during the work, DOE work was set up, so as to study the effect produced by the variation of the two main geometric factors that characterize this type of supports, and through an analytical model derive optimal values that can be used in subsequent productions. The two optimized functions, on which the effect of the above variations was studied, were the blade distortion with respect to the nominal model and the residue trace left by the support during mechanical removal. The work was conducted in collaboration with the company Avio Aero s.r.l. based in Rivalta di Torino (TO), which provided the necessary licenses and company know-how.

*“Alla famiglia,
agli amici.”*

Table of Contents

List of Tables	v
List of Figures	vi
Acronyms	viii
Introduction	1
1 Additive Manufacturing	3
1.1 Definition and classifications	3
1.2 History and development of technologies and companies	5
1.3 History and development of applications	8
1.4 Additive vs Traditional manufacturing: advantages and drawbacks.	11
1.5 Challenges and future directions.	14
2 Electron Beam Melting (EBM)	16
2.1 Machines and process description	16
2.1.1 Components	17
2.1.2 Commercialized machines	18
2.1.3 Process of layer construction	19
2.1.4 Process parameters	21
2.2 Physical mechanisms	21
2.2.1 Process defects in EBM	24
2.3 Metal powders for EBM	26

2.3.1	Gas atomization	26
2.3.2	Feedstocks materials	27
2.4	Comparison EBM - SLM	28
2.5	EBM applications	30
2.5.1	Arcam®	30
3	AM Process Chain	32
3.1	File CAD Generation	34
3.2	The STL file	34
3.2.1	Triangularization errors	36
3.3	Modeling of the scene	38
3.3.1	Positioning of the 3D model	38
3.3.2	Development of support structures	39
3.3.3	Slicing process and staircase effect	40
3.4	Post-processing	41
4	Industrial test case	43
4.1	Design Of Experiment	43
4.2	Definition of variables and levels	46
4.3	Modelling scene	49
5	Thermal simulation	51
5.1	Classification of EBM process simulation models	51
5.1.1	Uncoupled models	53
5.1.2	Coupled models	56
5.2	EBM Thermal Simulation Tool	57
5.3	Application to test case	59
6	Test execution	61
6.1	Build generation and post processing	61
6.2	Dimensional analysis	62
6.2.1	Comparison with nominal geometry	62
6.2.2	Data processing	65
6.3	Critical analysis of the results	69

Conclusions	76
A EBM machinery	80
Bibliography	81

List of Tables

1.1	AM advantages and drawbacks in terms of product and in terms of process	13
2.1	Settable and Non-settable EBM process parameters . .	22
2.2	Comparison between SLM and EBM main features . .	29
4.1	Doe levels and factors (representative values)	48
6.1	Data processing results	68

List of Figures

1.1	7 AM Categories, according to ISO/ASTM52900-15 . . .	5
1.2	Additive Manufacturing History Timeline (AMPower Report, 30 March 2021) [7]	7
1.3	Percentage of Industrial and Public Sectors using AM technologies (Wohlers, 2018).	9
1.4	Additive manufacturing timeline, (courtesy of Graham Tromans)	10
1.5	Comparison between AM and Traditional manufacturing. Manufacturing costs as a function of component complexity.	12
2.1	Schematic sketch of a PBF-EB system (Courtesy GE Additive)	17
2.2	EBM process steps	19
2.3	(a) Default settings (b) Contour only (c) Hatch only (d) Number of contour passes set to 5 (e) Single direction hatching	21
2.4	balling effect representation	23
2.5	Schematic of gas atomization system	26
2.6	from left to right:(a) compressor support case for a gas turbine engine, (b) gearbox,(c) acetabular cups produced by Arcam EBM technology, Ti6Al4V.	31
3.1	Stages of the AM process	33
3.2	comparison between the nominal CAD file and different resolution levels in STL triangularization	35

3.3	(a) Inverted normal vectors; (b) Not-aligned vertices; (c) Boundary edges; (d) Intersecting faces (e) Non-manifold edges; (f) Over-refined mesh	37
3.4	different placements of a specimen in a modelling scene	38
3.5	example modeling scene with supports	39
3.6	difference between direct and adaptive slicing methods .	40
3.7	different slicing directions	41
3.8	(a) Laser Shock Peening (LSP); (b) Laser Polishing (LP)	42
4.1	Contour supports on a turbine blade	46
4.2	DOE factors	48
4.3	original and short blade	49
4.4	Builds modelling 2x8 blades	50
5.1	types of thermal models of EBM simulation	52
5.2	Model configuration and boundary conditions.	55
5.3	thermal analysis of a low and a high blade	60
6.1	Measurement acquisition procedure	62
6.2	Blades comparison with nominal geometry	64
6.3	Residual traces of supports on the blade	65
6.4	Matlab script to extract data	66
6.5	Pareto chart on penalized average	70
6.6	Pareto chart on penalized average	71
6.7	Pareto chart on residual	71
6.8	Residual plots for penalized average	73
6.9	Residual plots for trace left by supports	73
6.10	Contour plot for penalized average	74
6.11	Contour plot for penalized average	75
6.12	DOE optimization setting, search for the optimal values	76

Acronyms

AM

Additive Manufacturing

EBM

Electron Beam Melting

RP

Rapid Prototyping

ASTM

American Society for Testing and Materials

FDM

Fused Deposition Modelling

SLS

Selective Laser Sintering

CAD

Computer Aided Design

LAM

Laser Additive Manufacturing

PBF

Powder Bed Fusion

BJT

Binder Jetting

MJF

Multi Jet Fusion

DSLM

Direct Selective Laser Melting

DC

Direct Current

MRR

Material Removal Rate

TPR

Total Penetration Range

SLM

Selective laser melting

CT

Computed Tomography

STEP

Standard for the Exchange of Product Model Data

STL

STereoLithograhly

ASCII

American Standard Code for Information Interchange

LSP

Laser Shock Peening

LP

Laser Polishing

CMP

Conventional Machining Process

DOE

Design of Experiments

FE

Finite Element

FVM

Finite Volume Method

Introduction

AM has in recent years had an increasing impact in the world of manufacturing. Entering the field of Industry 4.0 innovations, many companies have decided to adopt as their production or prototyping system one of the techniques that fall under the category of Additive Manufacturing. Avio Aero is one of the leading companies in this sector, and for years now has been working on innovation and research to implement, develop, and continuously improve the use of these technologies through a dedicated R&D team.

There are many best practices that can be cited, and to which brief mention will be made within the paper, but Avio Aero's AM manufacturing research efforts are focused primarily in the aerospace sector, which requires particularly lightweight components with elaborate geometries. The purpose of this thesis, in fact, is to optimize the manufacturing process of a particular aerospace component, a low-pressure turbine blade, which at the state of the art is produced by EBM, an Additive Manufacturing technique that is based on the layered melting of a metal powder bed.

The paper is divided into two main parts. The first part is basically a general overview of the state of the art, collecting and summarizing the most recent papers and results of the global research activity on AM, including the evolution and progress that has been made in recent years regarding these very recent technologies.

The second part, on the other hand, focuses on the application to the industrial test case mentioned above, explaining how the optimization work was set up, what parameters were decided to be studied, and what steps were generally taken to arrive at optimal values.



The present Master Thesis Project has been developed in collaboration with Avio Aero who has approved the content of this document. Avio Aero is “a GE Aviation business which designs, manufactures and maintains components and systems for civil and military aviation”. Among different plants across Italy, Poland and Czech Republic, the company’s headquarter and largest production facility is located in Rivalta di Torino (TO), while in Cameri (NO) in 2013 was inaugurated one of the largest factories in the world entirely dedicated to Additive Manufacturing. In 2017 Avio Aero, in collaboration with Polytechnic of Turin, created the Turin Additive Laboratory (TAL), or “a joint lab created to collaborate on strategic research topics for the aviation industry, such as identifying new materials for this production technology”.

For setting up and conducting the work, we thank Avio Aero’s R&D Team and the Turin Additive Laboratory (TAL), which enabled the execution and printing of the test cases, as well as provided the necessary measurement instruments and licenses.

Chapter 1

Additive Manufacturing

1.1 Definition and classifications

Additive manufacturing (AM) is a process used to manufacture mechanical components in an industrial setting. In opposition to traditional subtractive manufacturing technologies (milling machines or lathes), in which the final part is obtained by removing material from a solid block with the production of chips, AM focuses on the addition of material (layer by layer) to generate the component along a construction axis (z axis). The term also refers not only to the type of production but also to all business aspects related to it (economic, financial, logistical).[1]

Initially called 'rapid prototyping (RP)', the use of this term was later considered inappropriate by users, as the focus of the process changed with the evolution of technology. Over the years, in fact, the focus of companies has increasingly moved from simple prototyping to real production, and it is for this reason that, in accordance with the technical committee of ASTM International, the name additive manufacturing was adopted.[2] Additive manufacturing is also often

erroneously associated with the term '3D Printing'. The two names, however, are not interchangeable. 3D Printing, in fact, is a particular type of additive manufacturing based on the production of material layer by layer and is often used to refer to direct extrusion technologies involving polymers, such as fused deposition modelling (FDM). Another difference, moreover, concerns the type of focus on which the economics are based. While 3D Printing is focused on customized production, related to specific customer needs, the term additive manufacturing is used in the industrial environment, and focuses on large-scale production and fulfillment of company needs, with goals such as greater design freedom and lower prototyping and production costs.[3]

According to ISO/ASTM52900-15, there are seven processes recognized under the additive manufacturing category[4]:

- Vat photopolymerization: A vat of photopolymer resin is exposed to an energy source, such as a laser beam or digital light projector, which hardens the material layer-by-layer.
- Material extrusion: A material is deposited from an extruder onto a substrate. Typically, a thermoplastic filament is melted by a heating mechanism and extruded through a hot end.
- Material jetting: Specialty printheads, spray a liquid material onto a substrate.
- Binder jetting: A process by which a liquid bonding agent is deposited onto a bed of powder.
- DED: In which metal, as a powder or wire feedstock, is fed in front of an energy source, such as an electron or laser beam, mounted on a multiaxis robotic arm.
- Powder bed fusion: This is a process by which an energy source, such as a laser or electron beam, is directed at a bed of powder to heat the individual particles until they melt together.

- Sheet lamination: In this process, sheets of material are fused together, with the desired shape etched into each shape. The final object is then removed from the block of bound sheets.

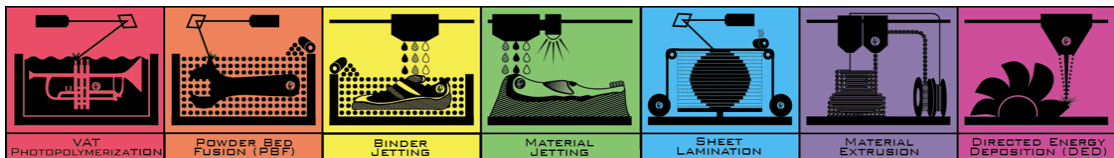


Figure 1.1: 7 AM Categories, according to ISO/ASTM52900-15

1.2 History and development of technologies and companies

AM was officially born in 1986, when the American engineer and entrepreneur Chuck Hull patented the Stereolithography technique and founded the ‘3D system inc.’, of which he is today still the CEO. Before him, some ideas on laser photopolymerization of liquid polymers had been patented, but nothing that could have a significant impact in the field of rapid prototyping. [5] In the same year Carl R. Deckard files a patent for the first SLS machine, that could melt small particles of plastic, metal, ceramic or glass powders into solid 3D forms with a high-powered laser.[6]

In 1989 Scott and Lisa Crump file for a patent for fused deposition modeling (FDM), a 3D-printing technology that applies materials in a series of additive layers by mathematically slicing and orienting models. Crump also establishes Stratasys, a 3D printing and production company. In the same year EOS, a company that use 3D printing with Selective Laser Sintering (SLS) technology generated from CAD software, is founded in Germany.

In 1997 AeroMat produces the first 3D printed metal process using laser additive manufacturing (LAM) that utilize using high-powered lasers to fuse powdered titanium alloys. Meanwhile a Swedish company named Arcam introduces for the first time the Electron beam melting (EBM), a metal additive manufacturing technology that uses an electron beam to melt layers of metal powder, ideal for manufacturing lightweight, durable and dense end parts. Some years later, in 2016, U.S. multinational General Electric will acquire the company with the goal of turning it into the leading edge of electron beam technology manufacturing for the GE Aviation Industry.[6]

In the early 2000s, AM evolved, and its use was increasingly impactful from an enterprise manufacturing and private use perspective. The birth of parallel projects such as ‘RepRap’, an open-source printer concept capable of self-replicating its component parts, has made more and more curious people interested in the technology. In 2009 the patent on FDM technology, previously held by Stratasys, expires. Since then, the cost of filament 3D Printers has become increasingly affordable, making them accessible to individuals, and the number of low-cost machines on the market has increased exponentially.[5] Over the next 5 years LB-PBF system supplier achieved continuous increase in system sales as many adopted the technology.

In the beginning of 2015, the first hype ended, and stock prices of traded AM companies declined significantly. However, system sales in metal PBF systems stayed strong as more industries, such as aviation, energy and gas and oil were adopting the technology. In 2016, Desktop Metal and HP entered the market and introduced their metal BJT technology. A second hype was created on the promise of significant increase in productivity in comparison to PBF. In 2019, first systems have been installed at beta customers.[6][5]

2021 was characterized by major technological announcements and acquisitions that were made especially by the large AM players. After a quite intense year of 2020, Stratasys has further broadened their spectrum of technologies with the acquisition of Xaar to step into the Thermal Powder Bed Fusion market and intensify the competition with HP and their MJF system.[6]

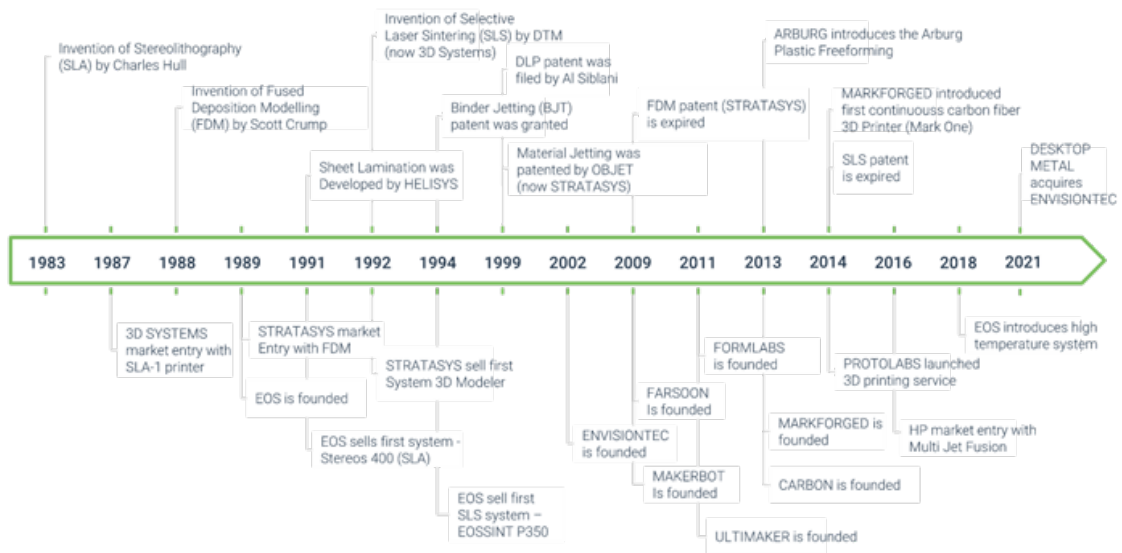


Figure 1.2: Additive Manufacturing History Timeline (AMPower Report, 30 March 2021) [7]

1.3 History and development of applications

The main applications of AM have changed over time. A study conducted by Deloitte (Cotteleer and Joyce, 2014) analyzed the applications of AM in the past, present, and future. Currently, the main applications of AM are changing to end product production, mass production, and democratized consumer 3D printing. According to the Deloitte study, the production of completed products via AM is expected to occur from 2030 to 2050 [8].

One of the very first application of AM was the rapid prototyping. Traditionally, 3D printing was a rapid prototyping technique for manifesting preproduction designs physically. As a prototyping technology, 3D printing can be a fast, more accurate method than handcrafting a design. Before investing in the expensive tooling and molds required for making large batches of goods, a 3D-printed prototype can be used to envision crucial design elements.[9] In 1993 Soligen Commercializes Direct Shell Production Casting. The company bases its technology on the Massachusetts Institute of Technology's patent for ink jetting a liquid binder onto ceramic powder to form shells that are then used in the casting process, giving rise to rapid casting [10]

Not long after, rapid tooling also began to be developed, using these technologies as secondary tools for manufacturing. For instance many processes are used to 3D print objects that will aid in the creation of metal parts, such as models for tooling and investment casting. Examples of tooling include the following: a mold that can be used to form an end part from raw material; a jig or fixture designed to hold a part in place while other steps in the manufacturing process are performed, such as drilling an assembly. [11]

In the early 2000s, the first application field in which additive is used is the automotive. The automotive industry has been using AM technology as an important tool in the design and development of automotive components because it can shorten the development cycle and reduce manufacturing and product costs. AM processes also have been used to make small quantities of structural and functional parts, such as engine exhausts, drive shafts, gear box components and braking systems for luxury, low-volume vehicles. The use of AM has proven to be fundamental also in the racing sector, where, unlike passenger cars, vehicles for motorsports usually use light-weight alloys (e.g., titanium) and have highly complex structures and low production volumes.[12]

Immediately after AM finds wide application in the aerospace industry as well. Aerospace components often have complex geometries and are made usually from advanced materials, such as titanium alloys, nickel superalloys, special steels or ultrahigh-temperature ceramics, which are difficult, costly and time-consuming to manufacture. Additionally, aerospace production runs are usually small, limited to a maximum of several thousand parts. All these reasons make the technology highly suitable for aerospace applications, for example to fabricate components for satellites, helicopters, and jet engines. Some of the most used solutions include the production of mixing nozzles, support cases, turbine blade with internal cooling channels, static turbines.[13] According to the latest market estimates, in recent years the application of AM in the aerospace sector has

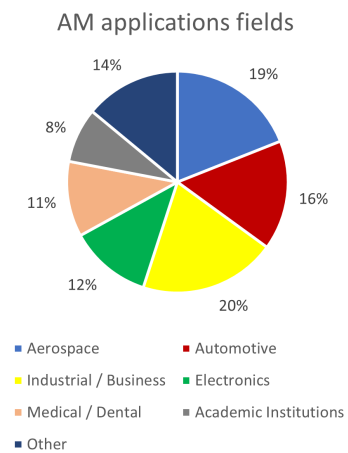


Figure 1.3: Percentage of Industrial and Public Sectors using AM technologies (Wohlers, 2018).

overtaken the automotive sector, occupying a slice of 19% of the market, compared to 16% occupied by the automotive sector. (Wohlers, 2018).[10]

One of the last fields in which AM has found application is biomedicine. In particular, AM technology provides new accurate and personalized ideas and methods for the diagnosis and treatment of orthopedic diseases (such as bone-arthrosis replication, implant customization, etc.) and the stomatology (such as making removable partial dentures metal bracket, completes denture, implant prosthetics, and oral deformity correction, etc.). A new paradigm of AM application in the biomedical industry, which will be developed by 2030, is the bio fabrication using biologics or biomaterials as building blocks to fabricate substances, devices, and therapeutic products through a broad range of engineering, physical, chemical and biologic processes.[14]

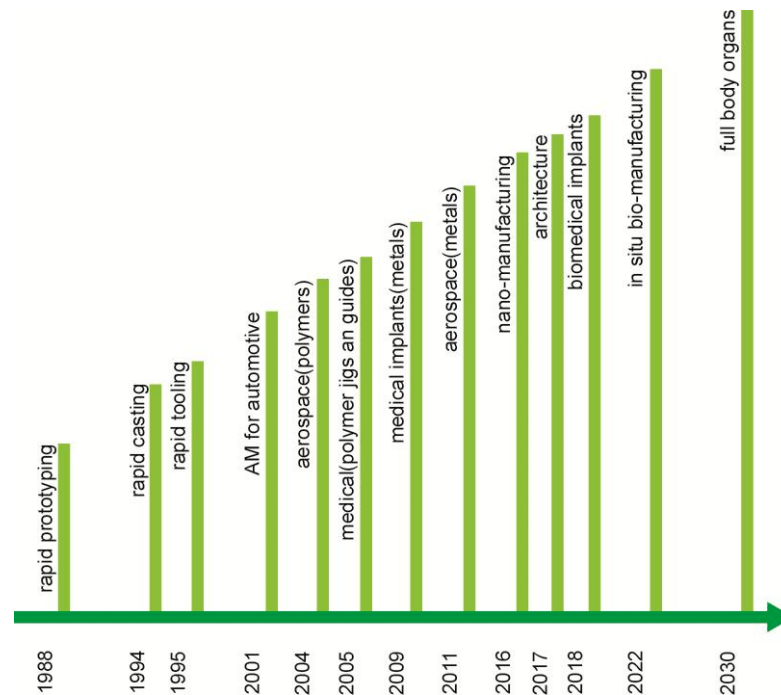


Figure 1.4: Additive manufacturing timeline, (courtesy of Graham Tromans)

1.4 Additive vs Traditional manufacturing: advantages and drawbacks.

Manufacturing regions can be categorically classified and defined by three key attributes: Complexity advantage, Customization and Volume. Complexity advantage is the final geometric complexity and feature location a manufacturing method can achieve. Customization is focused on the ease of feature and individualistic variability the manufacturing technology offers that makes a similar product unique to each other with a customizable feature. Volume refers to the production quantity of parts in an order or batch, whereby the production volume can range from singular to multiple parts.[1]

Lost cost high volume production has been the primary focus of traditional manufacturing industries. This is especially true for Mass Manufacturing: parts characterized by their simplicity and lack of customizability. The high capital investment required to create assembly and production lines using AM, does not make it a financially feasible investment for manufacturers. Conventional methods such as injection molding still dominate this space. The environment where AM works best, however, is low-volume manufacturing, characterized by high geometric complexity and high degree of customization. In a production of this type it is convenient to use AM because the geometric complexity and the customization are factors with little or no impact on the final cost, compared to the interference that the number of packages produced has instead. This is the concept of ‘Complexity for free’, which is very important in evaluating the economic impact of AM in companies. In traditional production, on the other hand, all three factors are significant, and the final cost grows exponentially in relation to them. The main part about the convenience for a company in using additive over a conventional process, then, is finding the break even point of the cost/piece – geometric complexity graph (figure 1.5). In

the graph, we can see how in the AM process the increase of geometric complexity in the piece is almost not at all impacting, in fact the curve associated with it is almost horizontal (the slight slope of the curve is given by the fact that there are supports, rejects and finishes).

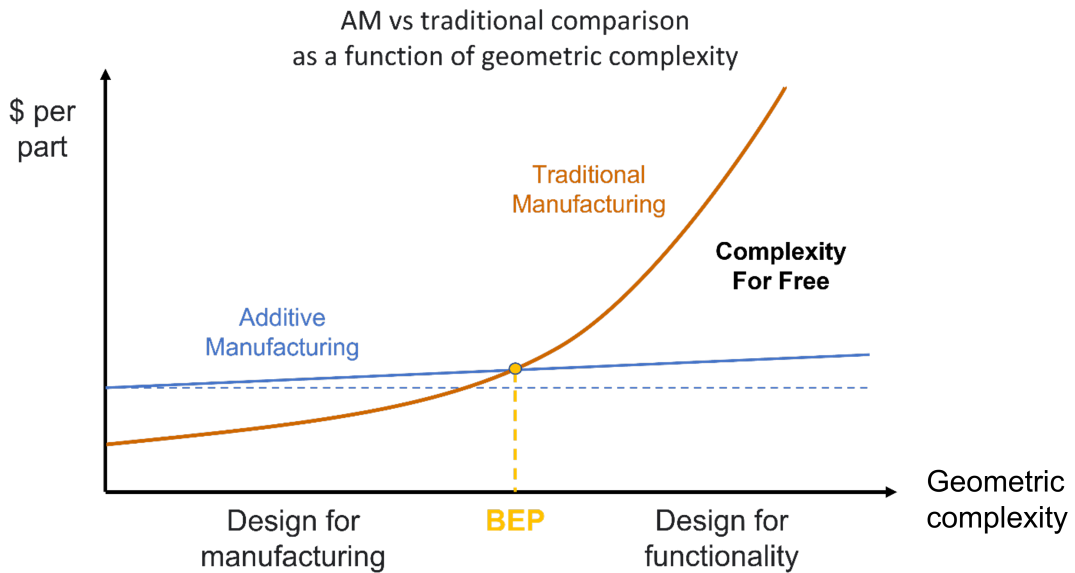


Figure 1.5: Comparison between AM and Traditional manufacturing. Manufacturing costs as a function of component complexity.

A common mistake is to equate the product of an additive manufacturing process with the end product of a traditional manufacturing process. In this way, at first impression, a part produced in AM (e.g., with metallic DSLM) may appear to be of lower quality than the equivalent obtained with traditional methods (e.g., turning). The error is not to consider post processing as an integrated part of the AM process. In this way, in fact, the equivalent of the piece that comes out of a DSLM machine is not a piece after turning, but the raw piece after the foundry process. So, both parts (the one produced in AM and the one produced using traditional methods) will require post processing and finishing, and the total cost of the two parts will be very close to each other.

The advantages and disadvantages of AM (summarized in table 1.1) can be classified in two ways: in terms of product and in terms of process. The first compare the end product of an AM process (including post processing) with the end product of a traditional production. The second, on the other hand, compare the entire supply chain, in terms of time and resources (from raw material to final product) of the two manufacturing methods.

	Advantages	Drawbacks
In terms of product	Maximum design freedom	Need for support structures
	Lightweight structures	Poor surface finish
	Possibility of integrating several parts into one	Limited number of materials
	Ergonomic tooling design	Cost of materials
	Strong customization	
In terms of process	One machine, unlimited shapes	Lack of automatization
	Lack of equipment	Low speed
	No locking devices	Limited number of materials
	Permitted undercuts	Limited work volumes
	Time and costs depend only on production volume and not on geometric complexity	Cost of the system
	Minimum operator intervention	

Table 1.1: AM advantages and drawbacks in terms of product and in terms of process

1.5 Challenges and future directions.

In the last decade, Industry 4.0 have attracted the attention of both academia and industry since it is considered as the major paradigm shift in the factories of the future. AM, as a key technology in the context of the forthcoming revolution, offers great potential for the prospective developments in this new era provided that some current barriers are overcome in the near future. [15]

Although AM technology recently has undergone significant development, it still is not widely accepted by most companies. Improving the technology to the point of changing this mindset and gaining industry acceptance, as well as broadening, developing and identifying manufacturing applications that are only possible with AM processes, are the critical targets for the next 5–10 years. [16]

Some of the key players in the AM ecosystem, to be developed in the future for these purposes, are:

- Design.
The unique capabilities of AM processes greatly enhance the freedom of designers to explore novel applications of this technology. However, it is not easy for designers to take advantage of these capabilities. To address this issue, in the near future there will be a need to develop a uniform method of design, methods for simultaneous product-process design, and methods by which to assess lifecycle costs and impacts of parts and products fabricated by AM. It will also be necessary to implement new foundations for computer-aided design systems with modular simulation capabilities, multiscale modeling and inverse design methodologies.
- Process modeling and control.
The ability to achieve predictable and repeatable operations is critical. Process variability must be reduced, as must the sensitivity

to process variations. To achieve this, there is a need for future research in the areas of Process-structure-property relationships, Closed-loop adaptive control systems, and new sensors (process, shape/precision/surface finish) that can operate in build-chamber environments

- Materials, processes, and machines.
Research opportunities in AM materials, processes and machines include a better understanding of the basic physics and chemistry of AM processes that capture complexities in the multiple interacting physical phenomena inherent in most processes, New open-architecture controllers for AM machines, exploitation of unique characteristics that differentiate AM from conventional manufacturing processes, screening methodologies for advanced manufacturable materials to answer why some materials can be processed by AM and some cannot, micro and nano research to develop better tools with which to build structures and devices atom by atom (nano-manufacturing), and the development of sustainable (green) materials, including recyclable, reusable, and biodegradable materials, to reduce environmental impact.

In accordance with the aforementioned Deloitte study of 2014 (Chapter 1.3), the different approaches on the future of AM by consumers are mainly two: some believe that AM technology will continue to be used primarily for prototyping applications, while others believe that AM technology can revolutionize entirely manufacturing processes. Regardless of one's viewpoint, there is little doubt that the past 30 years have witnessed an unceasing advancement in AM system functionality, ease of use, cost, and adoption across multiple industrial sectors. While there is still some time before AM realizes its full potential, companies should assess how AM can help advance their performance, growth, and innovation goals. [17]

Chapter 2

Electron Beam Melting (EBM)

2.1 Machines and process description

Electron beam melting (EBM) is a RP process, developed and commercialized by Arcam®, Sweden. It produces fully dense metal parts directly from metal powder, having the characteristic properties of the target material. The EBM system builds structures from the bottom up by scanning the focused electron beam to selectively melt specific powder areas. [18]

Using an electron beam to melt the metal powder beam, EBM is able to achieve very high melting temperatures, and thus process heat-resistant materials quickly and functionally, producing parts with excellent quality.

It is one of the latest AM techniques using a computer-controlled electron gun to create fully dense 3D objects directly from metal powder. Like other techniques using AM, this also creates objects layer by layer[19].

2.1.1 Components

The system can be broken down into the following hardware components (figure 2.1):

Build Chamber: The fabrication of the part actually happens in the build chamber. The chamber also houses almost all the mechanical components of the system including the build tank, powder feeders and raking systems.

Build Tank: build tank is literally a steel tank with a platform in the XY plane capable of moving along the Z-axis. The part is fabricated over a start plate that is pre-heated prior to the start of the build.

Powder Feeder Raking system: The powder is stored inside two hoppers located in the top left and right corners of the build chamber. The raking system picks up a calibrated dose from the two hoppers and spreads a thin uniform layer over the bed of powder in the build tank.

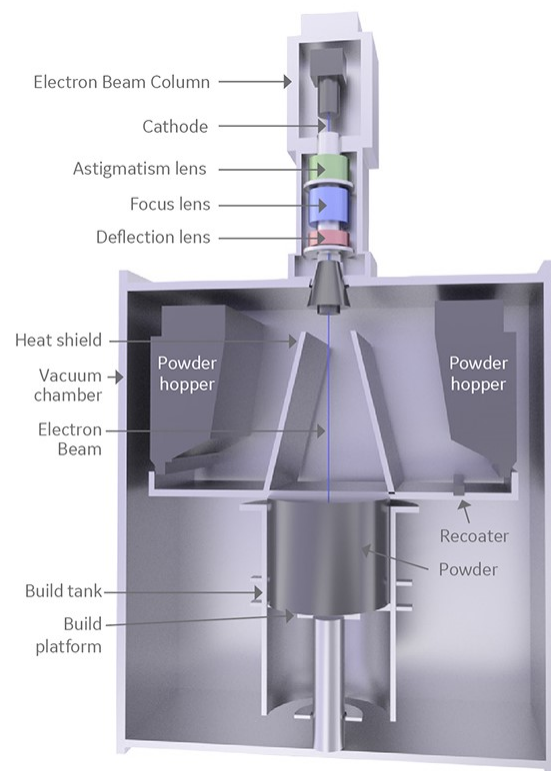


Figure 2.1: Schematic sketch of a PBF-EB system (Courtesy GE Additive)

Control System: the control system consists of a computer, programmable logic controller, signal amplifier and a DC power supply.

High Voltage Power Supply: the high voltage power supply located at the bottom of the control cabinet. It provides power to the following components: Heating the filament, Grid cup-filament bias voltage, Acceleration voltage for the electrons. Vacuum System: The build chamber is held between 10^{-3} and 10^{-4} mBar, while the electron gun between 10^{-7} and 10^{-6} mBar. These vacuums are achieved using two turbo pumps aided by a backing pump

The electron beam column: it consists of a cathode assembly, a drift tube-anode assembly, focus coils, astigmatism coils and deflection coils. The cathode assembly consists of a tungsten filament based cathode and a grid cup. A potential difference between filament and the anode, accelerates electrons from the filament towards the anode. The cross sectional geometry of the beam is controlled by the focus coils and the astigmatism coils. The position of the beam over the surface of the part in the build plane is controlled by a set of deflection coils. [19]

2.1.2 Commercialized machines

EBM machines were first commercialized by Arcam in approximately 1997 [6]. Arcam's S12 EBM system is the first commercial electron beam based layered manufacturing system designed for producing dense freeform metal parts. Subsequently, various lines of machinery were developed by the company in the years. They are customized according to the customer's needs, and depending on the type of application, features such as the size and shape of the build chamber may vary.

In Appendix A are some of the Arcam machines currently on the market with the main feature of each one. [20]

2.1.3 Process of layer construction

The build process begins with the heating of the start plate. The temperature of the start plate before the first layer is added is defined according to the powder material that has to be melted, and it is controlled by the added beam power. As mentioned above, the whole process occurs in a vacuum. The first melted powder layers form the base of the part. These layers together can form a solid foundation, or they can form a thin network-like structure that becomes the support structure on which the real part is built. Preheating of the powder bed takes place through a series of defocused beam passages at high power and high speed. The power and the scan speed are decreased in the subsequent melting step.

After the selective melting phase, the build table is lowered by one layer of thickness, and additional powder is delivered from the powder hoppers and then raked. The process is repeated until the part is completed. After building, the part is left to cool down under an increased helium pressure. At the end of the process, when the part is removed from the building chamber, a soft agglomerate powder adheres to the fabricated part and covers it completely. This agglomerate is called breakaway powder, and it is removed by means of sandblasting, using the same powder used in the EBM process. Since there is no minimum of oxygen uptake inside the build chamber during the melting process, the unused powder can be recycled several times without any alteration of its chemical composition or physical

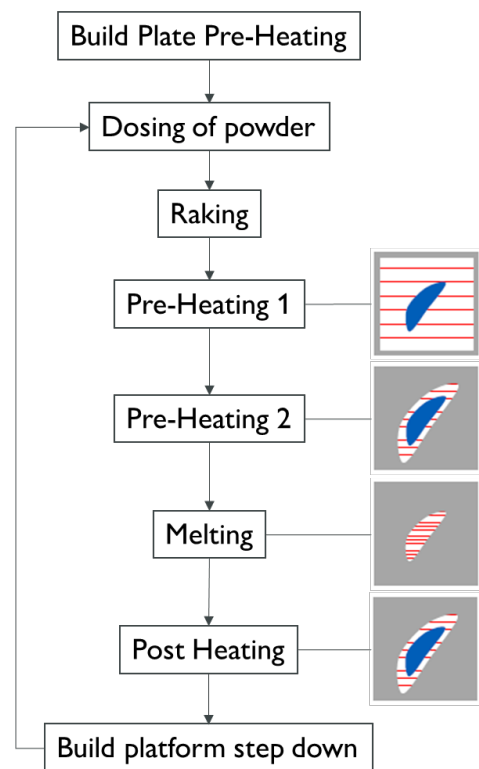


Figure 2.2: EBM process steps

properties. The building process steps in an EBM machine is depicted in Figure 2.2. The heating of the start plate, before that the first layer is deposited, is the first step of the process.

The different heating steps, throughout the whole process of layer construction, are divided into[21]:

- The Pre-heating phase: subdivided into two steps, it takes place through a series of defocused beam passages at high power and high speed. The first step, Pre-Heating 1, acts on the entire powder bed, whereas a second step, Pre-heating 2, is more focused around the geometry to be melted. The pre-heating of the powder brings numerous advantages to the process, such as the reduction of the thermal gradients between powder particles during the melting process, helping to avoid powder spreading and increasing also electrical and thermal conductivity of powder bed, improving the beam-matter interaction efficiency
- The melting phase: during this phase the power and the scan speed is decreased, and the electron beam is focused on the cross-section of the part to be melted and solidified. The most commonly used fusion themes are the hatch theme (figure 2.3 c) and the contour theme (figure 2.3 b), or different combination of the two depending on the direction of scanning and the percentage of use of one or the other (figure 2.3 a,d,e). Hatching creates the bulk melt and performs most of the melting process, using a beam with variable power and velocity to facilitate the heat dissipation and to prevent overheating. Contouring melts the perimeter of the part cross-section using a constant beam power and velocity, representing the barrier between the surrounding sintered.

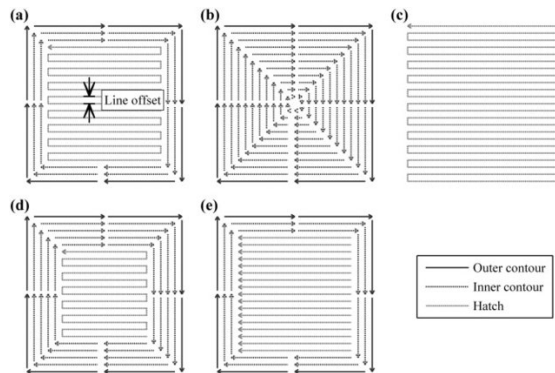


Figure 2.3: (a) Default settings (b) Contour only (c) Hatch only (d) Number of contour passes set to 5 (e) Single direction hatching

- Post-heating (or Ironing): this is an optional step, during which the layer is quickly scanned by defocused electron beam. Its main scope is to level out build temperature and to reduce the thermal gradients, obtaining, as much as possible, an even temperature distribution inside the build.

2.1.4 Process parameters

EBM process parameters can be divided into two categories: settable parameters, which can be set by the operator depending on the type of build, material, and other processing characteristics, and non-settable parameters, which are the physical characteristics of the process that affect machining and must be considered during the build preparation and process simulation stages. The main parameters, according to the distinction criteria just explained, are summarized in table 2.1.

2.2 Physical mechanisms

The main mechanism during the EBM build construction process is the interaction between the electrons and the powder bed. When the electrons hit the powder particles, a large fraction of their kinetic energy

The process parameters of EBM are:	The physical characteristics of the process are:
Beam current	Speed of electron under control of electric field
Pulse duration / Energy per pulse / Power per pulse	Specific power consumption
Accelerating voltage	Power requirement (P)
Focus offset (the additional current to translate the focal plane)	Material Removal Rate (MRR)
Layer thickness	Total Penetration Range (TPR)
Lens current	Power density
Spot size	
Scan speed, scanning mode, scanning strategy	

Table 2.1: Settable and Non-settable EBM process parameters

is released as thermal energy which melts, sinters, heats and vaporises the material. The remaining part of the kinetic energy is transformed into radiation and secondary electrons that leave the surface. It involves four main effects: the spread of particles, the sintering of particles, the melting of particles and the evaporation of some alloying elements. [22] The powder particle spreading, sometimes also referred to as puddling phenomenon, manifests itself as an explosion at the moment the electron beam comes into contact with the upper layer of the powder bed. The main causes that provoke this type of effect are hypothesized to be mainly three: residual water or humidity within the powder,

whose immediate transition from liquid to vapor state can cause an instantaneous and sudden release of energy, the momentum transferred by the electrons coming into contact with the metal, and the negative electrostatic charge of the powder causing a mutual repulsive force. These three effects can be mitigated through the use of expedients such as paying special attention during the atomization gas process to produce the powder (capitol 2.3.1), so as to reduce the residual humidity, increasing the size of the powder particles and acting appropriately on the pre-heating stage. Powder sintering depends on the amount of heat exchanged during the pre-heating and melting phases. The latter, in turn, depends on process parameters such as power beam, spot size and scan speed. Often the sintered powder at the end of the process also remains compact in the areas around or in close proximity to the melted zone. To remove this strongly compacted powder at the post-processing stage, a blasting operation using the same type of powder used during the process is sufficient in order not to contaminate the recovered material.

Particle melting is closely related to the concept of wettability. Wettability represents how well melting has occurred and how well the liquid portion has actually adhered to the underlying solid. It is measured by the value of the theta angle (figure 2.4),

which is the angle formed between the xy plane and the plane tangent to the surface of the melt. The lower its value, the greater the wettability of the powder. Ideally, the value of this angle should be zero. If its value exceeds 90 degrees, an effect called 'balling' is generated, which is very

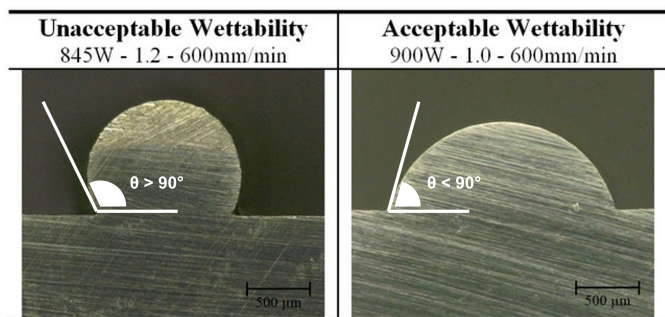


Figure 2.4: balling effect representation

damaging to the process and results in low quality of the final product. The wettability characteristics depend mainly on the temperature, the level of impurities and the contamination of the material. Since it is not possible to completely eliminate the latter two factors, slightly more power is often required from the electron beam than would be needed to melt a single layer, so that it can penetrate deeper by increasing the influence of the melt zone. On the other hand, one must calibrate the excess power well, because this is one of the main causes leading to the evaporation of alloying elements. In addition, the vacuum created in the machine lowers the evaporation temperature of light elements. For this reason, the final part and recycled powders may have a smaller amount of alloying elements than the initial powder. [23]

2.2.1 Process defects in EBM

Failure to keep on of the above effects under control can produce very common process defects when trying to produce a part in EBM:

- **POROSITY AND LACK OF FUSION**
Porosity is a major defect in additive manufacturing including EBM also. The main causes of are powder quality or poorly optimized parameters. During the process of quick solidification the gas remains trap in the form of bubbles or spherical voids.
- **BALLING**
As already mentioned, Balling effect, that is sometimes called Melt ball formation, takes place when molten powder do not solidifies into solid layers instead it solidifies in spheres melted metal solidifies into spheres (figure 2.4)
- **RESIDUAL STRESS, DELAMINATION AND CRACKING**
Residual stress is very natural in additive manufacturing process. It mainly occurs because the material undergoes through different temperature levels hence the change temperature gradient induced

the residual stresses in the manufactured parts. The defect of delamination is associated with residual stresses, and it is caused when the tensile stress in-between the two layers become more than their capacity of binding. Cracking mainly depends on the material and there may be many causes of its occurrence. One type of cracking is known as solidification cracking and it is caused by the residual stresses. The main cause of this type of cracking is the application of excess energy creating the forces in-between the liquid area of the pool and the areas that have been solidified.

- SURFACE DEFECTS

The two major indicators of the roughness of the finished part are the powder size and the diameter of the heating spot. There are two main phenomena that are responsible for the roughness of the surface, that are: Irregular edges of layers and the material surface roughness.

- GEOMETRICAL DEFECTS

The excess application of heat may cause the material to deform from its shape. The important geometries are manufactured by using the supports either thermal or mechanical. Swelling effect may also occur that is mainly responsible for solidification of the melt pool over the surface of the part. Warping is another type of geometrical defect. This is because the heating effect warps the substrate during the process.

- SMOKING

As in EBM the beam consists of electrons therefore, upon striking with the powder, it not only produces the heat but also the electric charge. Therefore, it is utmost important to optimize the electron beam before the start of the process because it is so crucial to avoid the static charge. When the electrostatic force exceeds the binding force in power, it causes the powder particles to disperse from the bed, causing the smoking effect. [24]

2.3 Metal powders for EBM

As mentioned above, PBF processes require metal powder as a raw material. The powder shape is generally spherical and the distribution of the size of virgin powders ranges between 45 and 100 μm while the size of the sieve mesh is usually 150 μm . The powder can be recycled without appreciable modification in chemical composition or physical properties. EBM systems can work with many classes of materials that include steels (17-4 and H13), Ni-based superalloys (625 and 718), Co-based superalloys (Stellite 21), low-expansion alloys (Invar), hard metals (NiWC), intermetallic compounds, aluminum, copper, beryllium, and niobium. γ -TiAl alloys are central for EBM applications, especially the intermetallic alloys, because to date they cannot be processed with any other process. The metallic powders for EBM process are produced by the gas atomization process. [25]

2.3.1 Gas atomization

Gas atomization is the process where the liquid metal is disrupted by a high-velocity gas such as air, nitrogen, argon, or helium. Atomization occurs by kinetic energy transfer from the atomizing medium to the metal. In gas atomization, a high-velocity gas jet disintegrates molten aluminum into droplets that solidify to form the powder. The material flow during atomization is vertically upward (also known as "updraught"). Molten metal of the appropriate composition is supplied from a holding or melting furnace at the required temperature to the

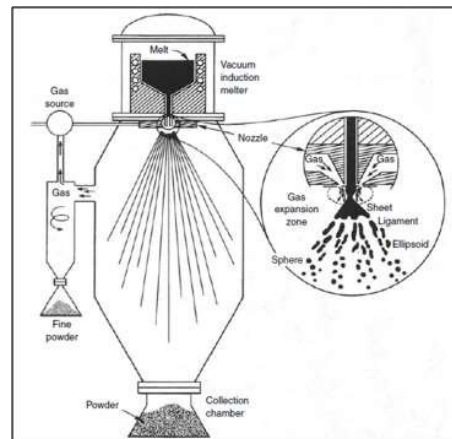


Figure 2.5: Schematic of gas atomization system

atomizing bay. The liquid is drawn from the bay through a liquid delivery tube into the atomizing nozzle. This is achieved by the aspirating effect (suction) caused at the nozzle end of the delivery tube by the flow of the high-pressure atomizing gas in the nozzle. When the liquid metal meets the high-velocity gas, it is broken up into droplets and sprayed as a jet. The droplets are quenched by the gaseous atmosphere in the chamber to solidify as powder particles. These particles, together with a substantial volume of cooling air, are then drawn through a chiller chamber into the collection system consisting of two sets of cyclones. After the cyclones, the powder is transported in an atmosphere of inert gas to the screens and pack-outs where they are packed under inert gas. [26]

2.3.2 Feedstocks materials

The choice of powder is a key factor in EBM production, both from the perspective of cost and the mechanical properties desired in the final product. The characteristics of the part, moreover, are influenced not only by the type of powder, but also by the way it is produced. As already specified, the morphology of the powder is a very important factor because it can influence surface roughness and porosity, or the presence of moisture or various impurities within it can give rise to phenomena such as balling or smoking. This is why EBM companies generally prefer to patent the raw materials as well, so that they have control over the entire supply chain and the assurance that the machinery sold has been tested with the respective powders. On the EBM side, Arcam has also patented its powder (Appendix A), which can be used specifically for each machine. Some of the most widely used, for the SPECTRA series and the Q series, are [20]:

- TITANIUM POWDERS

Ideal for a wide range of high-performance applications in aerospace, automotive and biomedical. Titanium is well-known for being

light alloys characterized by excellent mechanical properties and corrosion resistance combined with low specific weight and biocompatibility.

- **NICKEL-BASED ALLOY POWDERS**
Ideal alloys for high-stress, high-temperature aerospace, industrial manufacturing and oil gas environments. Nickel chromium superalloys like Nickel 718 and Nickel 625 produce strong, corrosion-resistant metal parts with excellent tensile, fatigue and creep.
- **STEEL ALLOY POWDERS** Ideal for spare parts, gears and tooling inserts across all industries.

2.4 Comparison EBM - SLM

Selective laser melting (SLM) is one of the new additive manufacturing techniques that emerged in the late 1980s and 1990s. During the SLM process, a product is formed by selectively melting successive layers of powder by the interaction of a laser beam. Upon irradiation, the powder material is heated and, if sufficient power is applied, melts and forms a liquid pool. Afterwards, the molten pool solidifies and cools down quickly, and the consolidated material starts to form the product. After the cross-section of a layer is scanned, the building platform is lowered by an amount equal to the layer thickness and a new layer of powder is deposited. This process is repeated until the product is completed. [27]

Despite being two very similar technologies, and both belonging to the powder bed fusion technical group, SLM and EBM have some substantial differences ranging from the type of process to the application of the final product. The main difference between these two technologies lies in the energy source, which is a laser beam for SLM and an electron beam for EBM.

Due to the use of electrons, EBM must work under vacuum, while an inert atmosphere is fed to the SLM chamber. An electron beam is generally of a much higher power, therefore, it usually works with larger powder particles and higher layer thickness. Also, significantly faster scanning rates can be used. Nevertheless, it does not necessarily mean that the EBM process is faster. In EBM, a pre-scan is applied to each layer to heat the powder up to reduce temperature gradients and great thermal stresses which would negatively affect part build-up (chapter 2.2.1). That prolongs the process. In SLM systems, only the building plate can be preheated, not the whole ‘powder bed’. SLM thus yields products with significant internal stresses, which are usually desirable to be removed by additional heat treatment of the products. After EBM, no heat treatment is generally necessary. [28] The comparison of the main features of SLM and EBM is given in Tab 2.2.

Energy source	laser	electron beam
Beam size	0.1-0.5 mm	0.2-1.0 mm
Scanning	galvanometers	deflection coils
Resolution	0.04-0.2 mm	0.1 mm
Accuracy	± 0.05 -0.2 mm	± 0.2 mm
Working environment	inert atmosphere (Ar, N ₂)	vacuum
Preheating	not present	Powder bed pre-heating
Layer thickness	30-100 μm	50-200 μm
Scanning speed	< 10 m/s	< 8000 m/s
Build rate	< 50 cm ³ /h	55-80 cm ³ /h
Surface finish	Ra 9-12 μm	Ra 25-35 μm
Residual stresses	high	minimal
Heat treatment	stress relief required	not required

Table 2.2: Comparison between SLM and EBM main features

2.5 EBM applications

Some of the advantages of the EBM process are that it is capable of producing high quality metal parts comparable to those produced with traditional manufacturing methods such as casting, and that the parts produced not only possess high mechanical properties, but typically also have a high density (over 99%), thanks to the preheating process and the high temperatures required during printing. Preheating the build plate also minimizes residual stress, a common problem faced with metal AM, reducing the need for support structures. For these and other reasons, EBM finds numerous potential applications in aerospace, aeronautics and automotive systems, that can benefit from this density-compensated strength and stiffness.

2.5.1 Arcam®

Arcam applied its EBM system to produce functional parts for end users. Some of these applications included commercial and military aircraft, space applications, missiles and various subsystems (e.g., engines and accessories) which use light-weight materials such as titanium alloys. For example, an EBM-produced compressor support case for a gas turbine engine using Ti6Al4V is shown in Fig. 2.6 a.

Ti6Al4V open cellular foams fabricated using EBM demonstrated high potential for novel applications in automotive systems too, due to their light weight and exceptional mechanical properties. EBM was used with this material to produce parts such as gearboxes 2.6 b, suspension parts and engine parts with lattice structures for race cars. A titanium aluminide alloy with low density and high specific strength (ratio of elastic modulus vs. density) and stiffness (ratio of yield strength vs. density) was also investigated using EBM for its potential to fabricate automotive engine components (e.g., engine exhaust valves and pistons).

Finally, another sector where EBM is widely applied is the biomedical sector. Arcam has applied EBM to manufacture a wide range of implant types such as acetabular cups (Fig. 2.6 c), hips, knees, shoulders and spinal implants, and a number of implants have been certified on the market. For example, using Arcam EBM technology, Adler Ortho Group launched the CE-certified Fixa Ti-Por acetabular cup in the European market in 2007, and more than 2000 of these cups have been implanted. Another fast-growing area for these applications is the dentistry business.[17]



Figure 2.6: from left to right:(a) compressor support case for a gas turbine engine, (b) gearbox,(c) acetabular cups produced by Arcam EBM technology, Ti6Al4V.

Chapter 3

AM Process Chain

Before arriving at the final product, the AM process goes through various steps from design to production to post processing (Figure 3.1):

1. Development phase: in this phase, the file is generated that will then be transferred, via memory card or other types of physical media, to the machine. It starts with the generation of the CAD model, functional for the required application, which is then simulated in the application and optimized for AM production. Then, based on this, the actual working environment is modeled on the machinery used.
2. AM Production phase: this is where the actual production phase of the part begins. Starting from the powder, using the process described in chapter 2.1.3, the layer-by-layer construction of the part takes place. Before this, a machine control operator sets all the parameters (chapter 2.1.4) and during the molding phase makes sure that there are no errors in the procedure. At the end of this stage, the blank is extracted from the powder.
3. Post processing Phase: this phase starts with the raw part extracted from the machine, which, through manual procedures, is cleaned of excess powder. Then it goes through various types of mechanical

processing, as needed, to remove supports and generally all those parts necessary for production but not functional for the application. Then, before the component can be called suitable, we make sure that it meets all regulatory standards through various types of quality tests.[29]

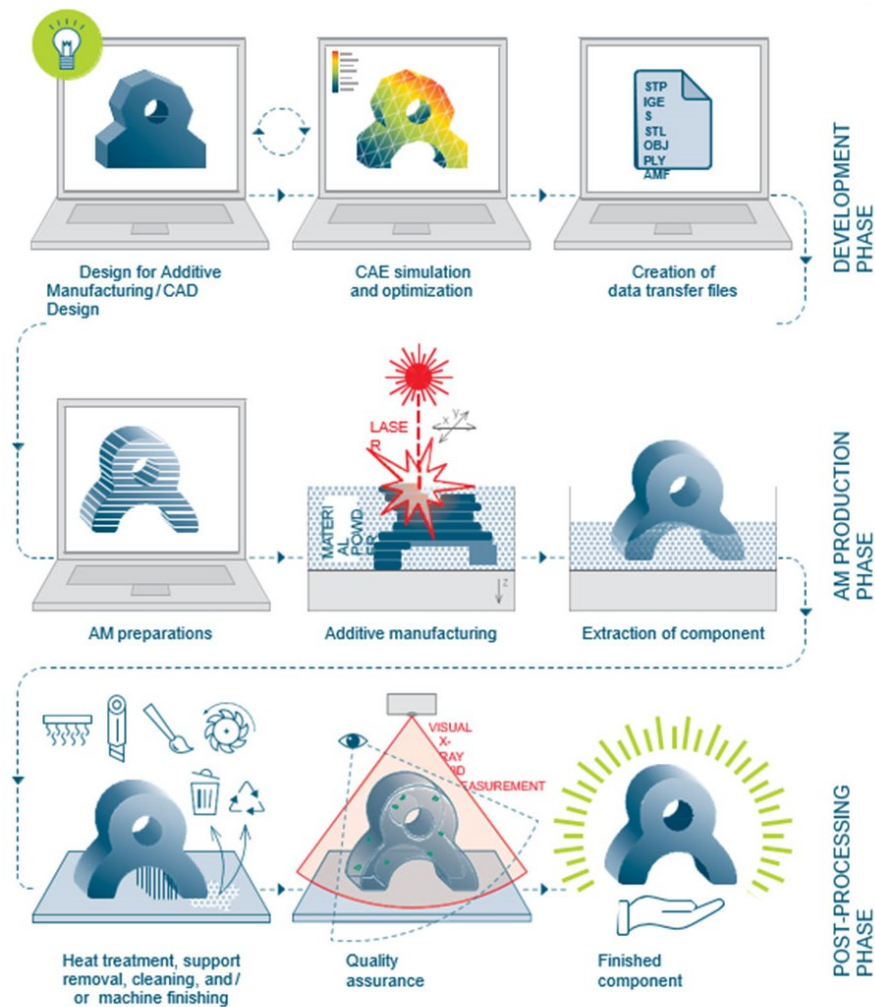


Figure 3.1: Stages of the AM process

3.1 File CAD Generation

The generation of the CAD file of a product developed in AM is based on how the product itself should look and function. It usually begins with a product idea, a 2D image such as a photograph, a set of 2D images like those derived from Computed Tomography (CT) scans, or a physical 3D object like a prototype or a part for reverse engineering. These are transformed into digital models (e.g. volume models or facet models) using solid modeling, metrology, or image reconstruction software. New software formats have been developed and standardized to support AM data preparation and digital workflow. For example, the AMF format, which has native support for color, materials, lattices, and constellations, has been standardized. Other formats such as STEP, STEP-NC, and 3MF have integrated AM concepts to compete with AM-specific formats.[30]

3.2 The STL file

STL is the native file format of 3D Systems' stereolithography CAD software. STL is an acronym for STereoLithography, which was 3D Systems' first commercial AM technique in the 1990s. "Standard Triangle Language" and "Standard Tessellation Language" are two backronyms for STL. Many additional software programs accept this file format, which is commonly used for fast prototyping, 3D printing, and computer-aided manufacturing. STL files simply define a three-dimensional object's surface geometry, with no representation of color, texture, or other standard CAD model features. Both ASCII and binary formats are specified in the STL format. Because binary files are smaller, they are increasingly prevalent.[31]

It works by deleting any building data, modeling history, and other information from the model and approximating the model's surfaces

with a series of triangular facets. Using a three-dimensional Cartesian coordinate system, an STL file defines a raw, unstructured triangulated surface by the unit normal and vertices (arranged by the right-hand rule) of the triangles. All STL coordinates were required to be positive values in the original standard, however this requirement is no longer enforced, and negative coordinates are now widespread in STL files. The units are arbitrary and there is no scale information in STL files. [32]

The STL file format is used by nearly every AM technology, and it is considered a standard. Most CAD software allows you to select the minimum size of these triangles, and the goal is to ensure that the models you produce don't have any visible triangles on the surface. The minimal distance between the plane represented by the triangle and the surface it is designed to represent is used to determine the triangle size. To look at it another way, a good rule is to keep the minimum triangle offset under the resolution of the AM machine.

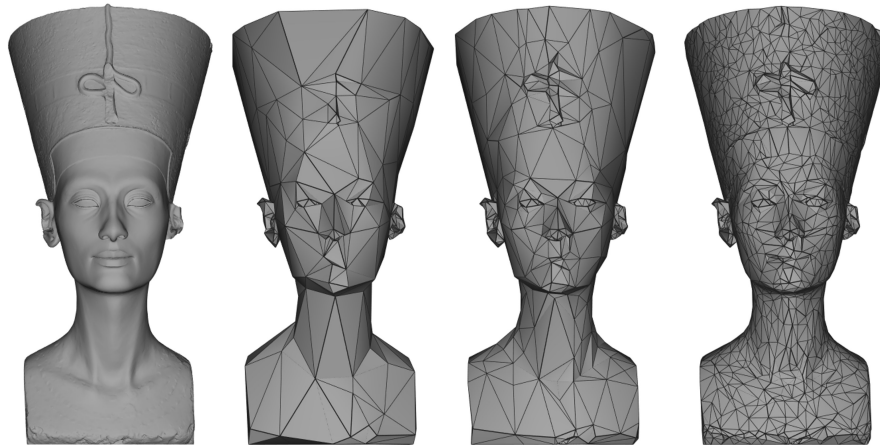


Figure 3.2: comparison between the nominal CAD file and different resolution levels in STL triangularization

3.2.1 Triangularization errors

Although most CAD programs make the conversion to STL process automated, there is a chance for mistakes to occur during this stage. As a result, a variety of software tools have been created to detect and, if feasible, correct such problems. When there are issues with the STL file that may prevent the component from being constructed correctly, STL file repair software, such as the MAGICS software from the Belgian company Materialise, is employed. When analyzing the CAD or the resulting STL data, it may be difficult for a person to spot such issues due to complicated geometry. If the defects are minor, they may go undiscovered until the part has been assembled. As a result, such software may be used as a check stage to guarantee that the STL file data is free of errors before the build begins. While most problems may be discovered and corrected automatically, there may be times when personal involvement is required. Because geometries can grow quite complicated, it may be difficult for the program to determine if the output is an error or part of the original design intent. [33]

The most common triangularization errors, when converting a CAD file to stl, are:

- Inverted normal vectors: Because STL is basically a surface description, the files' related triangles must point in the right direction; in other words, the surface normal vector associated with the triangle must specify which side of the triangle is outside vs. inside the component.
- Not-aligned vertices: Triangle vertices that are not aligned correctly might be caused by complex and extremely discontinuous geometry. Gaps in the surface may emerge as a result of this. Various AM technologies may respond to these issues in a variety of ways. Some machines may be able to bridge the gaps by processing the STL data. However, this bridge may not reflect the required surface, and

it's possible that the part contains additional, undesirable material.

- Boundary edges: Boundary edges are detected if some edges of the STL file are not connected to only one face. This essentially means that the model has holes and does not represent a closed surface.
- Intersecting faces: Intersecting faces are detected when two surfaces collide with each other. This error is commonly encountered when multiple bodies are occupying the same space.
- Non- manifold edges: Non-manifold edges are detected when more than two faces are connected to the same edge. An extra surface may be defined in the interior of the model, essentially splitting it into two.
- Over-refined mesh: A mesh is "over-refined" when the total number of triangles of the STL mesh is larger than required. This will not lead to any errors during 3D printing, but it will unnecessarily increase the size of the STL file, making it more difficult to handle.

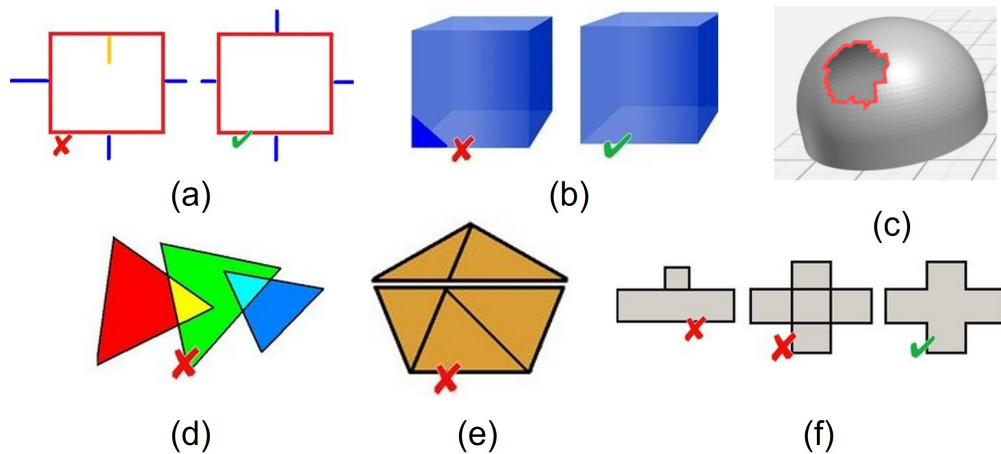


Figure 3.3: (a) Inverted normal vectors; (b) Not-aligned vertices; (c) Boundary edges; (d) Intersecting faces (e) Non- manifold edges; (f) Over-refined mesh

3.3 Modeling of the scene

After the STL file has been created and any problems produced by CAD model conversion have been corrected, a sequence of procedures must be completed in order to produce information that an AM machine can utilize to begin the build process. The right positioning of the 3D model on the construction platform, the development of essential support structures, and the slicing process are all included in these phases. Obviously, they are interdependent, so the supports required vary based on the orientation of the pieces on the build platform, and the surface quality, which is connected to the slicing phase, might improve or decrease.

3.3.1 Positioning of the 3D model

The visualization tool in most AM software lets the user to examine and alter the part's STL file. It might be resized, moved to a specific location on the construction platform, or oriented correctly if necessary. There are basically three criteria for machine positioning, on which the

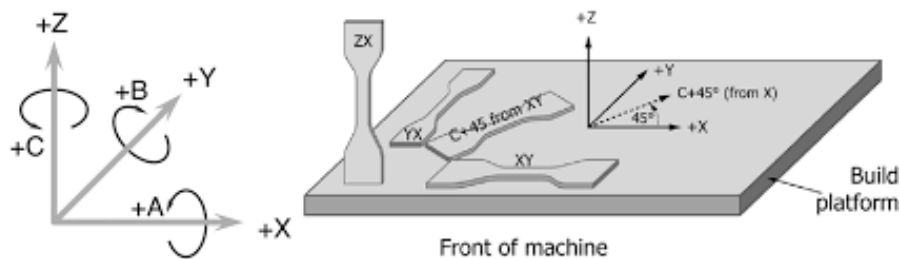


Figure 3.4: different placements of a specimen in a modelling scene

designer relies to model the scene and choose the orientation of the parts[34]:

1. Optimize the printing speed: a part with an extended projection in the xy plane will be faster to print than the same part that instead runs along the z axis.

2. Reduce the impact with the recoater by rotating the parts slightly around the z-axis so that contact with the metal part can occur gradually.
3. Reduce the Staircase effect (Chapter 3.3.3).

Together these three criteria define the orientation of the part in space, which can then be based on the experience of the designer or on the automatic calculation of the software, setting which of these three elements to give more importance to and which less.

3.3.2 Development of support structures

Supports must be placed to the part depending on the orientation. They are modelled using different ways. They may be created using CAD software and then exported as an STL file, or they can be made automatically in an AM software environment. In the first case, the part's orientation must be decided beforehand, and designing an ideal structure requires a great deal of skill. The second method offers more versatility as well as the ability to automatically position the component in line with optimal support structures. The role of the software is to automatically add support to all those parts where the plane tangent to the surface forms with the xy plane an angle less than the minimum angle to support. The minimum angle to be supported must be set by the designer in the software settings and depends on the process and the type of material (e.g. minimum angle to be supported for Ti6Al4V EBM is generally 30°) [35]

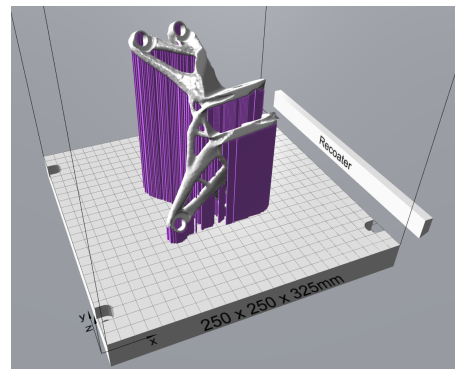


Figure 3.5: example modeling scene with supports

The EBM 3D printing process involves high temperatures, which can be a problem for parts. If they are too hot for too long a time, they can distort. This is the main reason EBM requires supports, whose main function is to provide paths for excess heat to “go away” and not to provide mechanical stability.

3.3.3 Slicing process and staircase effect

The STL model is sliced by a series of parallel and horizontal slicing planes based on the required layer thickness once the component has been suitably orientated along the construction direction and the support structures have been produced. Figure 3.6 shows two possible slicing procedures that can be used: direct slicing and adaptive slicing. The STL file is cut into layers of consistent thickness in direct slicing. Slicing is done in the Adaptive method by adjusting the thickness of each layer to the curve of the portion.

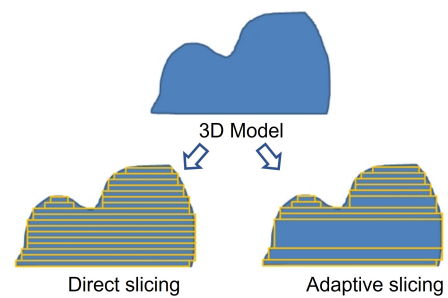


Figure 3.6: difference between direct and adaptive slicing methods

Staircase effect is a phenomenon associated with the slicing when the layer marks become distinctly visible on the surface of the parts, giving the perception of a staircase. This error is one of the most common drawbacks of layered manufacturing and has significant effect on shape accuracy and surface quality of fabricated models. Staircase effect cannot be eliminated, though we can diminish its influence as much as possible by choosing appropriate layer thickness and slicing orientation. Theoretically, smaller layer thickness corresponds to lower staircase effect, higher surface accuracy, and more fabrication time. However, being limited to the current production precision, thickness can only be adjusted in a certain range. Given the layer thickness, slicing orientation then becomes the one and only determining factor of staircase

effect. Apply different orientations, the same one inclined plane will result different errors, consequently, achieve different surface qualities. As shown in Figure 3.7, for the same facet F , three slicing orientations (d_1 , d_2 , d_3) generate three different volumetric errors ($e(a) > e(b) > e(c)$). In the case of AM, the slicing direction corresponds to the z

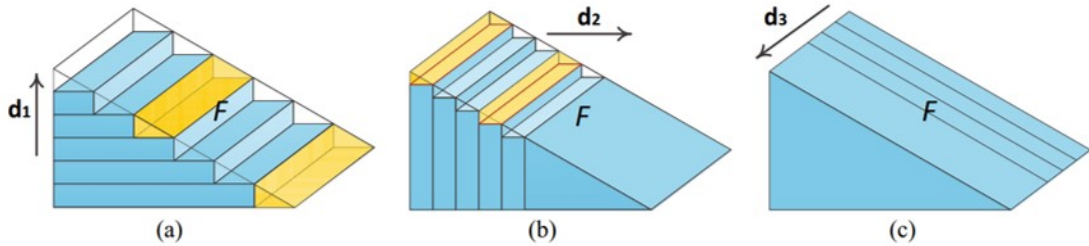


Figure 3.7: different slicing directions

axis of the modeling scene, and therefore to the construction direction of the machinery perpendicular to the planes in which the powder is spread.[36]

3.4 Post-processing

The removal of the component from the build plate and the removal of support structures from the build part, using milling, wire EDM, or other metal cutting techniques, are the minimum required post-processing steps, regardless of the AM technology used to produce a part and the application it is designed for.

In addition to these standard procedures, in the post processing of the piece developed in AM they can use various traditional mechanical and thermal finishing techniques:

- Laser Shock Peening (LSP) (figure 3.8 b)
LSP is a lateral expansion procedure that involves the material's plastic compression perpendicular to the surface. The ability to withstand transverse strain leads to the accumulation of local

compressive stresses when laser peening is done on thick or restricted objects. The heated zone, using a focused laser beam on the metallic surface for 30 ns, reaches 10,000 °C, resulting in plasma formation. The generated plasma absorbs laser energy until the laser-material interaction time is attained. Shock waves transmit the pressure generated by the plasma to the material. LSP is usually applied to extend the fatigue life of any component.

- Laser Polishing (LP) (figure 3.8 a)
LP is a technique to improve the surface roughness of AM-ed parts. When the laser energy irradiates the material surface during LP, morphological apices quickly attain the melting temperature. Due to gravity and surface tension, the liquified material reorganizes to the same level after the melt pool is generated. The heat-affected zone (HAZ) temperature lowers rapidly once the laser beam stops scanning the surface, resulting in melt-pool solidification and reduction in surface roughness.
- Conventional Machining Process (CMP): Milling, Rolling, Chemical Machining and Abrasive Machining
CMP is the traditional manufacturing process employed to enhance the manufactured parts' dimensional accuracy and surface quality. Owing to the popularity and acceptability at a wide level, they are also employed in AM for the post-processing of manufactured parts.[37]

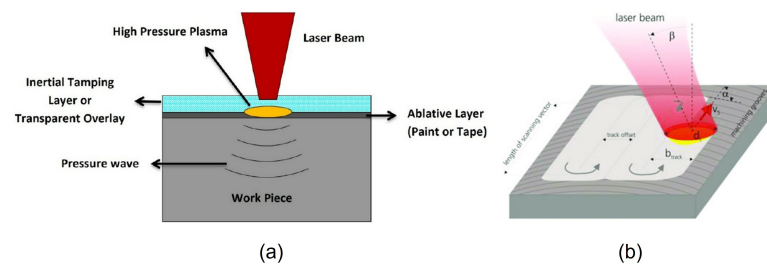


Figure 3.8: (a) Laser Shock Peening (LSP); (b) Laser Polishing (LP)

Chapter 4

Industrial test case

4.1 Design Of Experiment

Design of Experiments (DOE) is a statistical technique for set and define the parameters of any experimental testing activity. It became popular in the 1990s and was invented as a method for maximizing information from experimental data. Specifically, it is a statistical method that enables the planning, organization of experiments and thus proper and efficient data acquisition. Incorporating statistical considerations into the design of experiments can reduce trial development time, use available resources more efficiently, and achieve greater reliability of results.[38]

Considering experimentation as merely a test phase aimed at verifying whether the practical implementation of a new process/product meets the objectives set in the design phase may be reductive. In fact, experimentation can bring added value if it is thought of not only as a confirmation of what was planned but also as a potential source of improvement opportunities that cannot be guessed at beforehand. [39]

Often in the industrial environment, the complexity of phenomena prevents full control of the factors under investigation and complete

theoretical knowledge: this means that the cause-and-effect relationship between the factors affecting the process under investigation and the variables to be optimized is not always known a priori. Therefore, with the use of DOE, experimental techniques can be optimized, and more complex cases can be examined.[38]

The DOE method consists of 4 main steps:

1. Problem formulation.

The first stage of experimental planning involves problem definition. At this stage, the following aspects must be defined:

- Responses: these are the properties of the studied system that you want to optimize. The measured responses must be representative quantities of the properties of interest and must necessarily be provided as a numerical value, even when the survey is planned according to a qualitative scale, this must be appropriately transformed into a quantitative scale so that the results can be subjected to analysis.
- Independent factors or variables: these are the experimental variables that influence responses and are made to vary with each experiment. The choice of variables is a delicate balancing act. The study of many variables may entail conducting many experiments; on the other hand, the exclusion of some variables will risk thwarting the study if they turn out to be important and highly influential. Both quantitative and qualitative variables can be considered as factors.
- Levels: the values that each controllable factor can take are defined as levels. Generally, a normalized scale is used so that each factor is made to vary in the range of -1 to +1 while zero represents the midpoint.
- Experimental domain: experimental area investigated, defined by the intervals in which the experimental variables are made to vary.

2. Choice of experimental design.

The second stage of a DOE planning is the choice of the most appropriate design for the problem under investigation. The chosen design is associated with the mathematical model that will be used to describe the system. Defining the objective, that is, the purpose of an experiment, is critical in determining structure of the experimental plan. If the purpose is to extract from the data the preliminary information about the process under consideration, then a simple model capable of providing rough indications will be adopted; if, on the other hand, the purpose is the search for optimal experimental conditions then the plan should involve the use of a design capable of providing a detailed description of the system by means of a more flexible, higher-degree equation.

Experimental designs fall into 3 categories:

- Screening: ideal when studying a new process (or devising a new method); sometimes it may not be known in advance which, among many possible factors, might influence the response. So, one tries to screen out the most influential factors. Many factors can be handled with this approach, ranging from 5 to 12
- Optimization: requires more knowledge of the domain to be explored and a more elastic equation (with second-degree terms) to effectively model the response surface. Usually, 3 levels are considered for each factor, but 5 levels can also be used.
- Mixture: mixture designs allow variables that are not inherently independent to be investigated. In the case of wanting to optimize a formulation, variables are expressed in percentages.

3. Implementation of testing.

Once the experimental plan has been chosen, one can proceed to go to the laboratory or production line to carry out the established tests. Immediately thereafter, data analysis can be done by giving

the regression algorithms the experimental matrix along with the values of the response variable. To understand the validity of the model, an effective method is to plot the response values obtained from the model together with the actual values: if the values deviate greatly (high residual values) or show peculiar trends, errors may have been made or some effects neglected. At this point, one can construct the response surface, visualize graphically what the optimum condition is, and evaluate its stability.

4. Optimization

Optimization, which is the last step of DOE, is that stage where, not only do you go to optimize your process, but you can turn new knowledge into more effective decisions and more innovative processes for the future.

4.2 Definition of variables and levels

The purpose of this thesis work is to optimize the design of a particular type of supports, called 'contour' type supports, currently used in the production of low-pressure turbine blades using the EBM process. Contour supports are automatically generated using MAGICS software, and in turbine blades they are used to support mainly the areas where overhang is most pronounced. They are generated, at the CAD level, as surfaces, which are then interpreted by the machine as fins with thicknesses equal to the lowest possible resolution (roughly comparable to spot size).



Figure 4.1: Contour supports on a turbine blade

They are attached to the part by toothed shaping, to facilitate their removal during post processing. The first step for optimizing these supports, therefore, involved formulating the problem and choosing the experimental design. Therefore, the following aspects were defined, which are specified in chapter 4.1:

- Responses: it was agreed that the output worth studying the most, in this first phase of experimentation, was the maximum displacement of the part, that is, how much the supported part deviated from the nominal geometry during the production phase. As detailed in 2.2.1, there are many reasons why the final EBM production part deviates from the ideal geometry, which can range from an incompletely supported surface to the warping effect due to poor heat removal from the part to powder defects such as poor wettability or errors in the casting process. The purpose of this DOE is to study the effect of support design on the first two reasons just mentioned.
- Independent factors variables: Since there have already been various backgrounds on the use of these supports in the application case, it was decided to choose two main variables, which in the experience of the designers were the ones that could most influence the displacement of the part:

TOP LENGTH: top tooth length of the contour support at the point of attachment with the workpiece. The lower this value, the smaller the supported perimeter.

CONTOUR OFFSET: offset length between one surface and the next of the support. The lower this value, the denser the support will be, the greater the portion of the surface supported.

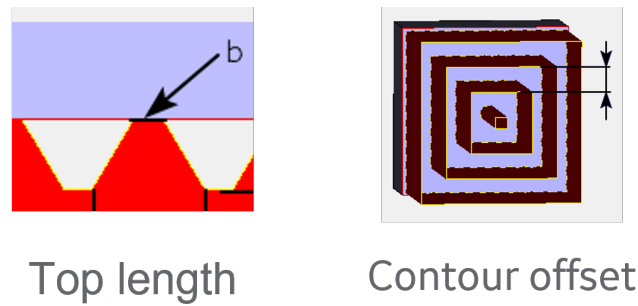


Figure 4.2: DOE factors

- Levels: again, as these supports have already been used several times in production and having ascertained that they do not cause any particular criticality, it was chosen for an experimental 'Optimization' type design, with four levels considered for each of the two variables.
- Experimental Domain: the variation domain of the levels was defined on the basis of experience-based considerations, starting from how the two parameters are used in the state of the art, balancing the more 'safety' variations, (those that were thought to generate a more stable structure), with more 'risky' variations, (those that were thought to go instead to negatively affect the stability of the part).

Level	Top length	Contour offset
1	a1	b1
2	a2	b2
3	a3	b3
4	a4	b4

Table 4.1: Doe levels and factors (representative values)

4.3 Modelling scene

The supports of a low-pressure turbine blade placed on an aeronautical turbofan engine (Figure 4.1) are the Test Case on which the DOE technique has been conducted once the parameters indicated in section 4.2 have been established.

The turbine blade has several key features:

- The blade section that is placed into the disk positioned on the shaft is referred to as the dovetail. It's a key zone since it's necessary to provide proper force transmission from the blade to the shaft while avoiding relative motion with the disk.
- Shank: Because angle wings are present, it must ensure that no flow leaks towards the disk.
- The part of the blade where the flow expands, changing its pressure and velocity is known as the airfoil.
- Shroud: it prevents leaks from forming near the tip of the turbine, which reduces its performance.

In order to accelerate the production process, since the blades were intended for research purposes only, it was decided to generate specimen blades from them, called 'short-blades', lower than the original ones, obtained by reducing the airfoil size and leaving all other characteristics unchanged. These blades - specimen, certainly not functional for production, are instead very useful for the intended purpose of the research through DOE, since they allow to speed up the construction

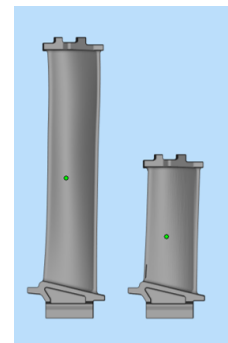


Figure 4.3: original and short blade

process, save material, and still evaluate the effect of max displacement on the main characteristics of the blade that are influenced by it, which according to previous studies turn out to be the dovetail, the shank and the shroud.

Having had the opportunity to print two builds, a factorial DOE was opted for, so as to analyze all possible combinations of level variation between the two factors. The total number of trials to be done for such a DOE, defined the two variables and the four levels, is $4^2=16$ trials in all. Therefore, two builds with eight blades each (8x2) were chosen. Thus, each blade has different configurations of the two parameters specified in 4.2. The blades were arranged within the scene based on the empirical considerations also specified in chapter 3.3.1. The dovetail height between each blade is staggered to reduce the volume occupied within the chamber, and the blades are rotated 8 degrees with respect to the x-axis to reduce the area of impact with the recoater. Before making these changes in the scene modeling, the reasoning was that the specimens would not affect each other in terms of the features to be studied, keeping the DOE variables independent.

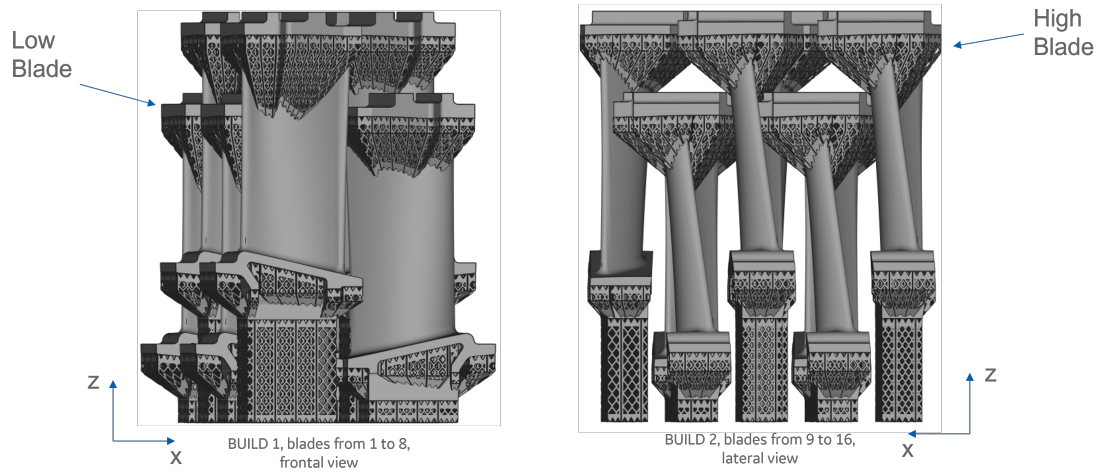


Figure 4.4: Builds modelling 2x8 blades

Chapter 5

Thermal simulation

5.1 Classification of EBM process simulation models

As illustrated in Figure 5.1, the many models for EBM process simulation that are currently available in the literature may be divided into three groups based on their level of approximation. These three categories include black box models, grey box models, and white box models. The more processing power and running time are required, and the more complicated and adaptable the model is, the lower the level of approximation[40]:

- Black box model: it is the most approximate model and solves a numerical problem without referring to any underlying physics. This model usually takes the form of a set of transfer parameters or empirical rules that correlate the outputs to a specific set of process parameters as inputs of the model
- Grey box model: less approximate than the black box, the level of approximation varies according to the number of approximations introduced into the model, that is, the number of process parameters that are considered in the modelling and which are correlated

directly to the process. In a grey box model, some or all the mechanisms that describe the process are known, but not all are fully represented in the modelling.

- White box model: it contains a great deal of detailed information, and thus no level of approximation needs to be introduced.

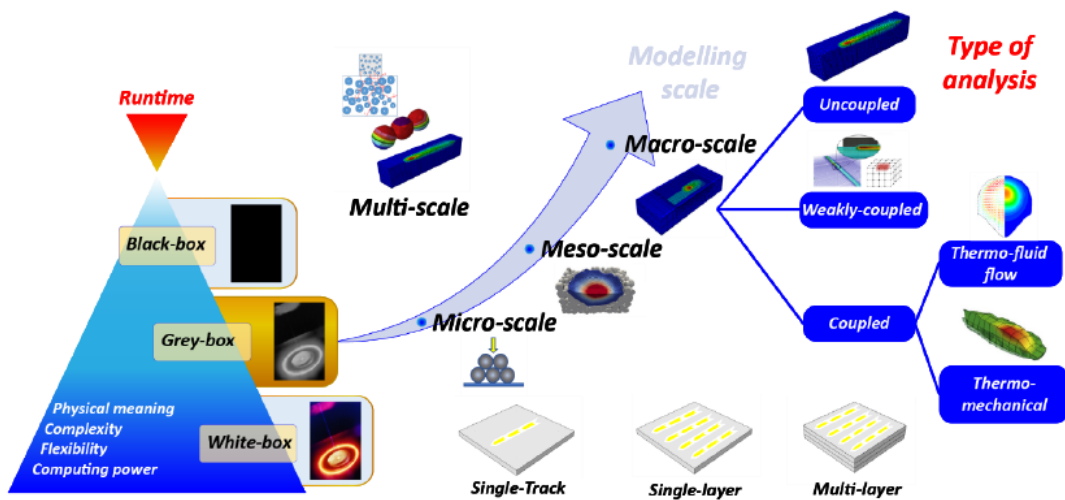


Figure 5.1: types of thermal models of EBM simulation

Another important distinction is made based on the scale considered and how the powder is modelled. In fact, to simulate the real trend, the powder can be modelled[41]:

- As a cluster of individual particles: in this case the scale to be considered is divided into micro-scale (single particle), meso-scale (area affected by the melt pool) and macro-scale (entire powder bed). This type of model results to be very accurate, but it requires a lot of computing power, large memory space and long processing time.
- As a continuum: a model more commonly used in the practice, because although less accurate it requires less computing power

and can give an idea of the thermal distribution in the part. It consists of considering the powder bed as a continuous body and discretizing it by the finite element method. depending on the scale considered, elements of different types can be used: 1D - considering the single track of the laser passage, 2D - considering the single layer, 3D - considering the multitude of layers from the buildplate up to the one we are studying.

In both distinctions, models of the various scales can be merged in a multiscale approach.

A final distinction, depending on the physical phenomena considered in the mathematical model, can be made between uncoupled and coupled models.[41]

5.1.1 Uncoupled models

Uncoupled thermal models only include phenomena that are primarily associated to heat transfer. Heat dissipation caused by viscous forces convective fluxes is ignored to simplify the study, and the material's wettability is always considered to be ideal. Thermal equilibrium is considered in an uncoupled heat transfer study to calculate the temperature distribution.

The equations defining this model are:

- The Fourier's law:

$$\mathbf{q} = -k\nabla T \tag{5.1}$$

where \mathbf{q} is the heat flux vector, k is the thermal conductivity (which is function of temperature), and $T = T(x_1, x_2, x_3)$ is the temperature, function of time and space both.

- The energy density equation:

$$e = cT + \Delta h \tag{5.2}$$

where c is the specific heat and Δh is the latent enthalpy.

- The heat losses due to radiation:

$$q_{\text{rad}} = \varepsilon \sigma (T^4 - T_{\text{room}}^4) \quad (5.3)$$

where ε function of T , is the emissivity, while σ is the Stefan-Boltzmann constant.

The heat loss due to convection could be neglected as the EBM process is performed under a high vacuum. The typical FE model consists of a thin single layer modeled as unsintered powder on the top of a substrate, representing this one the solid bulk already processed. The dimensions of the mesh are lower on the top layer respect to the substrate, and they decrease within and in the proximity of the portion of the powder layer where the heat flux is applied. The model configuration is illustrated in Figure 5.2, where Ω represent the top layer surface and Γ a circle portion of the top surface on which the electron beam is applied. T_{preheat} and T_{room} are respectively the preheating temperature and the build chamber temperature, T_{hs} is the inner heat shield temperature, while the heat flux q identifies the energy source.[21]

Writing the energy balance per unit volume within an infinitesimal control volume:

$$-\nabla \cdot \mathbf{q} = \rho \frac{De}{Dt} \quad (5.4)$$

where $\rho = \rho(T)$ is the density and t the time. Combining the equations (5.1),(5.2) and (5.4) we obtain:

$$c\rho\dot{T} = \nabla \cdot (k\nabla T) \quad (5.5)$$

Furthermore, to solve this heat transfer problem, a set of initial and boundary conditions must be defined. To impose that the temperature of the analyzed layer must be equal to the pre-heating temperature:

$$T(x_1, x_2, x_3, 0) = T_{\text{preheat}} \quad \text{with } (x_1, x_2, x_3) \in D \quad (5.6)$$

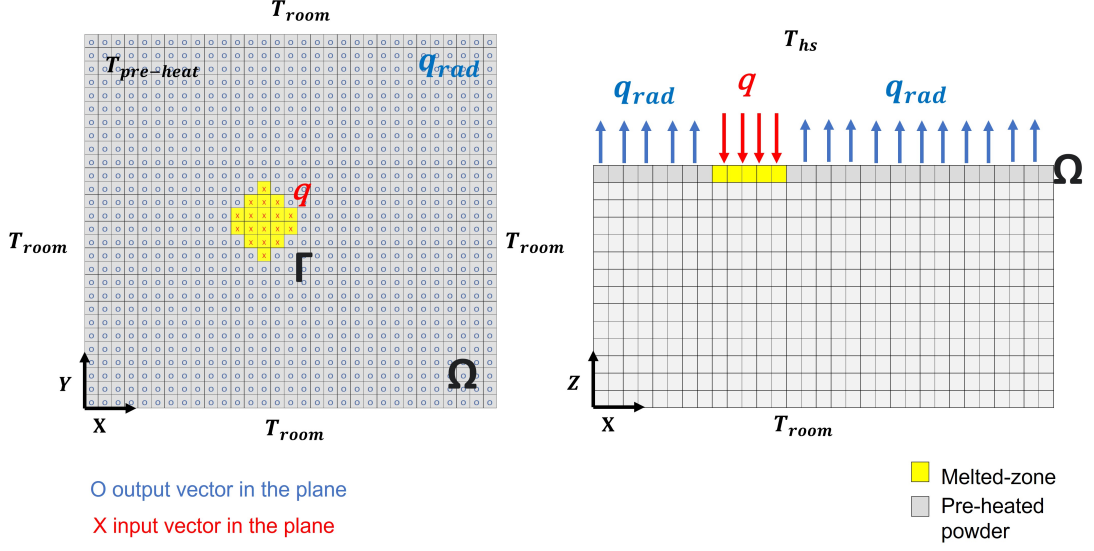


Figure 5.2: Model configuration and boundary conditions.

where D represents the union between the substrate and the layer domains. To impose constant temperature inside the chamber throughout the process:

$$T(x_1, x_2, x_3, 0) = T_{\text{room}} \quad \text{with } (x_1, x_2, x_3) \notin D \quad (5.7)$$

$$T(x_1, x_2, x_3, \infty) = T_{\text{room}} \quad \text{with } (x_1, x_2, x_3) \notin D \quad (5.8)$$

Finally, by imposing the boundary conditions for the melted zone:

$$-k \frac{\partial T}{\partial n} \Big|_{\Gamma} = q - q_{\text{rad}} \quad (5.9)$$

$$-k \frac{\partial T}{\partial n} \Big|_{\Omega - \Gamma} = -q_{\text{rad}} \quad (5.10)$$

combining all these equations, we get the following system:

$$\left\{ \begin{array}{l} C_P \rho \dot{T} = \nabla \cdot (k \nabla T) \\ T(x_1, x_2, x_3, 0) = T_{\text{preheat}} \text{ with } (x_1, x_2, x_3) \in D \\ T(x_1, x_2, x_3, 0) = T_{\text{room}} \text{ with } (x_1, x_2, x_3) \notin D \\ T(x_1, x_2, x_3, \infty) = T_{\text{room}} \text{ with } (x_1, x_2, x_3) \notin D \\ -k \frac{\partial T}{\partial n} \Big|_{\Gamma} = q - q_{\text{rad}} \\ -k \frac{\partial T}{\partial n} \Big|_{\Omega - \Gamma} = -q_{\text{rad}} \end{array} \right. \quad (5.11)$$

which, solved for each discretized element, provides the thermal trend of the part

5.1.2 Coupled models

Thermal-fluid flow models

The effects of flow convection on the melt pool shape and temperature distributions are considered in a thermal-fluid flow model. The model is based on laser welding process analytical modeling and takes into consideration the impacts of loose powder on fluid convection inside the melt pool [40].

This model also ignores momentum, bed shrinkage due to sintering, and radiation losses, but adds viscosity forces and hence Marangoni convection flows in the energy conservation equations to achieve a balance between the shear force and surface tension on the top surface of the molten pool.

By ignoring convection fluxes inside the melt pool, the pure thermal model indicates a narrower width and shorter length of the melt pool itself, as well as deeper penetration and a greater maximum temperature [41].

Thermomechanical models

The thermal model is modified in a coupled thermomechanical model by taking into consideration the material's mechanical characteristics, which are temperature dependent and allow for the computation of residual stresses inside a component throughout the simulation of the EBM process [41].

In order to account for the material's mechanical behavior, thermal strains are added to the solution of the equation (5.1), resulting in a contribution to the total nominal strain, which is made up of three terms:

$$\varepsilon = \varepsilon_e + \varepsilon_{pl} + \varepsilon_T \quad (5.12)$$

The elastic (e), plastic (pl), and thermal (T) stresses are represented by the variables in the equation. When it comes to the thermal strain, the following equation is used to calculate its increment:

$$d\varepsilon_T = \alpha dT \quad (5.13)$$

Where α is the coefficient of thermal expansion. The equilibrium produced by the governing equation should be satisfied by the solution of the elasto-plastic problem created by these strains:

$$\nabla \cdot \sigma = 0 \quad (5.14)$$

in which σ represents the nominal stresses.

5.2 EBM Thermal Simulation Tool

The thermal model on which the tool that was functional to carry out this work is based is a gray box, multi-scale uncoupled model, which allows to analyze both single and multiple layers. Starting from the equations (5.11), for simplicity and computational speed, is assumed

to have for each build layer a periodic heat flux Φ and a time-averaged temperature \bar{T} , with a periodicity given by the total layer time t_{layer} []. By means of these assumptions, the Eq. (5.11) becomes:

$$\begin{cases} \nabla \cdot (k \nabla \bar{T}) = 0 & \text{in volume,} \\ \hat{n} \cdot k \nabla \bar{T} = \bar{\phi} - \epsilon \sigma (\bar{T}^4 - T_{hs}^4) & \text{on top,} \\ \hat{n} \cdot k \nabla \bar{T} = -\epsilon \sigma (\bar{T}^4 - T_{amb}^4) & \text{on sides and bottom.} \end{cases} \quad (5.15)$$

By further assuming:

$$\bar{T}^4 \approx T^4 \quad (5.16)$$

Eq. (5.15) turns into the static heat equation. Assuming a surface pixelized in equally large pixels of area A_{pixel} , an energy

$$E_i = \sum_{\text{process steps } j} E_{i,j} \quad (5.17)$$

is applied to the pixel i during the processing of a layer. $E_{i,j}$ is the energy into pixel i during process step j as obtained from beam data. From this, a corresponding time-averaged heat flux ϕ_i into pixel i is calculated as

$$\phi_i = \frac{1}{t_{\text{layer}}} \frac{\alpha E_i}{A_{\text{pixel}}} \quad (5.18)$$

where α is an electron absorption coefficient. Solving Eq. (5.15) with the assumption (5.16) and with heat fluxes as obtained by Eqs. (5.17), (5.18) the temperature distribution in the build surface can be simulated. The heat equation is solved using the Finite Volume Method (FVM). The computational domain is discretized in voxels, hex elements (cubes), which are added layer by layer as the build proceeds. Each voxel has its own physical properties, namely thermal conductivity k and relative emissivity ϵ and their size is adaptive based on temperature difference. To decrease computation time, neighboring voxels can be merged into a larger one in an octree structure.[42]

5.3 Application to test case

The tool described was used for the purpose of the thesis work to accomplish the thermal analysis of the two builds (Chapter 4.3). As mentioned, in order for the DOE work to be effective, it must be made sure to vary only the parameters studied, keeping every other type of production parameter as similar as possible from specimen to specimen, or in this case from blade to blade. Therefore, one of the parameters that has gone to be studied with the thermal analysis is the temperature trend along the blade, verifying that in all sixteen blades produced the trend and the average temperature were as close as possible to each other.

What we wanted to particularly test was that the position inside the chamber and the presence of different types of supports did not vary significantly in temperature. A significant variation in temperature, in fact, could have meant a greater or lesser incidence of the warping effect (Chapter 2.2.1), which thus risked increasing the distortions on the overhang parts and adversely affecting the study.

The analysis was carried out for all sixteen blades, and after comparing the results, both graphically and numerically, it could be seen that no notable differences in temperature along the xy plane transpire. A slight difference appears, on the other hand, between the blades placed on different z-heights (high and low blades, chapter 4.3), but not significant enough to have noticeable impacts on the total distortions (we are talking about differences on the order of 10 K, compared with temperatures of 1200 K and above). This is probably due to the fact that, starting all the supports from the buildplate, the higher blades have more elongated supports, extending further along z, and therefore a greater presence of heat-dispersing material. In Figure 5.3, the thermal trends of a low blade and a high blade are shown (all others are identical, depending on how they are positioned on the z axis). The

x-axis zero represents the bottom layer of the blade (relative reference system). It can be seen that for the first few layers the trend is almost identical. The minimum point of the curve represents the geometrically largest section of the dovetail, which is also the one with the greatest heat loss. As one moves up along the airfoil, the two curves become closer together, until they become virtually identical again at the top of the shroud. In both blades, an average temperature of 1168 K is found. Therefore, it can be said, with some margin of error, that the position within the build, both along xy and along z, and the different conformation of the supports, do not significantly affect the thermal distribution within the part, and therefore can be ignored as DOE parameters. It was possible to verify these results later in the work, through the study of the effects that transpire from the Pareto chart (figure 6.5).

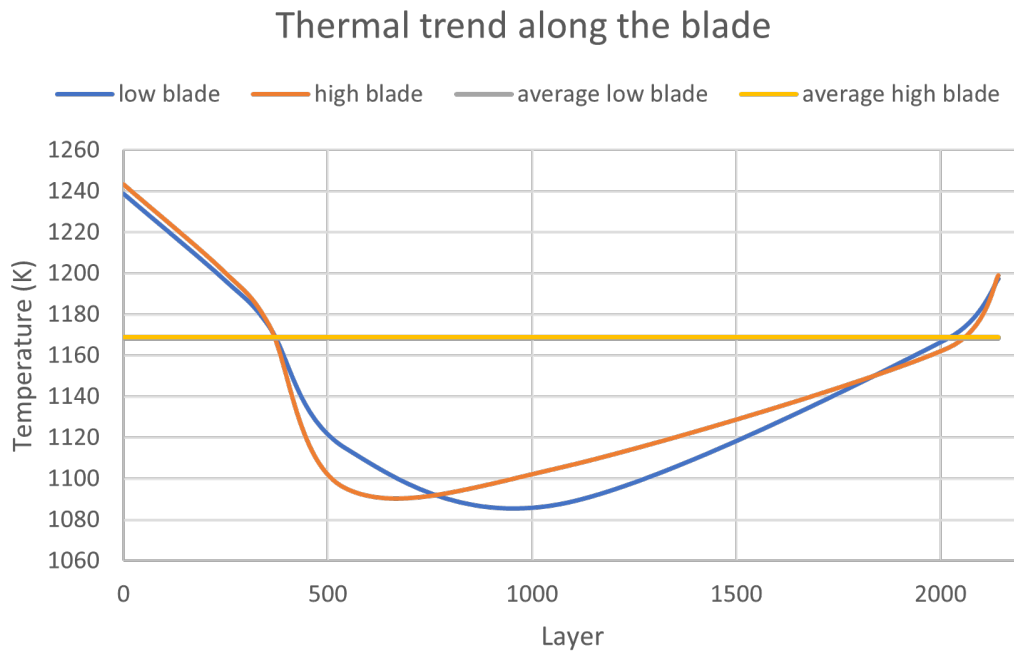


Figure 5.3: thermal analysis of a low and a high blade

Chapter 6

Test execution

6.1 Build generation and post processing

Once the two builds were modeled (Chapter 4.3), the turbine blades were printed in Ti6Al4V through an EBM Spectra H machine. The first post-processing actions involved powder removal through compressed air. This was followed by sandblasting, to remove the more compact powder deposited on the part, using the same powder contained within the chamber, so as not to cause contamination and to be able to reuse as much material as possible. Mechanical removal of the supports was then carried out. The removal was performed manually by a blade-by-blade operator, the work was supervised, and scores were assigned based on the timing and difficulty of removal. During the removal phase, it was noted that the supports with lower contour offset were the most difficult to remove, both in terms of timing and the residue left on the blade. In contrast, supports with higher contour offset were much easier to remove and left very little residue. It quickly became clear, therefore, that the lower the contour offset, the denser the supports, the greater the difficulty of removal. The quality of the blade itself is also affected, since considerable traces of residue are present, it is

necessary to apply additional post-processing operations to bring the surfaces in line with the desired quality standards. Of course, since it is not the purpose of this work, the only operation implemented is the one just described of manual removal of the supports, but it was noted that for the purposes of qualitative analysis of the part not only the distortions of the geometry, but also the trace of residue left behind could impact the critical analysis of our DOE results.

6.2 Dimensional analysis

6.2.1 Comparison with nominal geometry

Dimensional analysis was conducted using GOM comparison software. Using a laser scanner, 16-point clouds were acquired (one for each blade), which were then imported in the software. The procedure for the analysis is as follows:

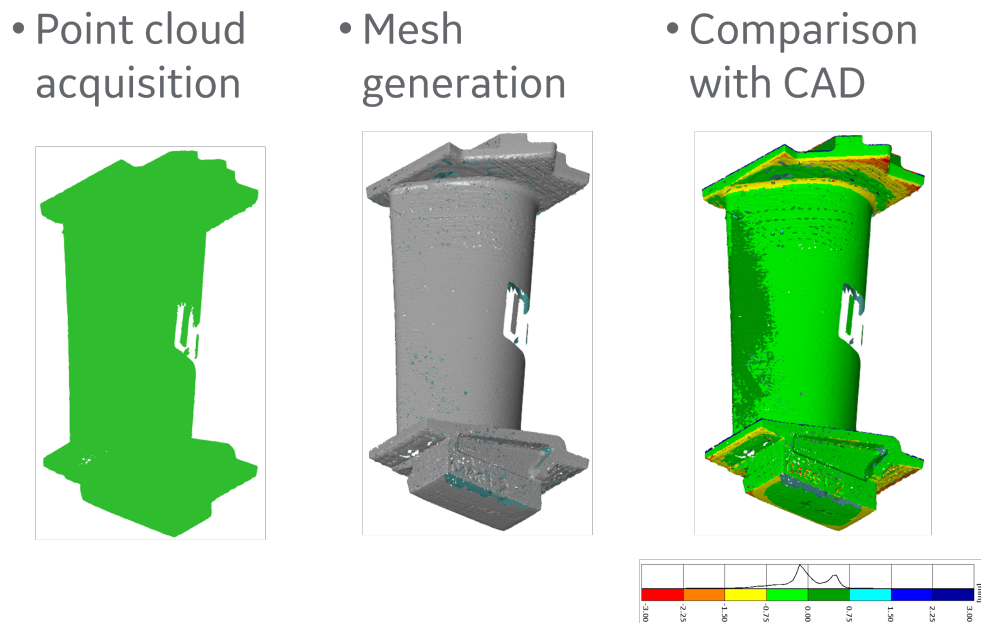


Figure 6.1: Measurement acquisition procedure

1. Automatic mesh reconstruction based on the point cloud. In the case of the blades, the mesh was incomplete in the central area of the airfoil. This derived from the fact that when the measurements were conducted, this area was used as the laser-scanner arm attachment zone. Understanding that, based on experience, the airfoil is the area least subject to distortion, this choice was implemented in order not to influence the measurement of the most distorted areas too much.
2. Reversal of normal vectors and mesh cleaning. By reconstructing the mesh as a shell, the software automatically highlights the directions of the surface normal vectors. Typically, the coloring is as follows: gray highlights the areas of the mesh with positive normal vectors (the outer surfaces of the shell), and green highlights the areas with negative normal vectors (the inner areas). It may sometimes happen that the two normal vectors are reversed. It is therefore important to act manually, highlighting the areas with inverted normal vectors and using the appropriate command. This step is especially crucial for the subsequent alignment steps.
3. Surface smoothing. Through this command, you smooth the surface of the mesh, making it more or less regular depending on an error that can be input manually. Through smoothing, you eliminate any background noise that may have been there during cloud acquisition, and thus make sure that small areas with large distortions are not considered in the final analysis.
4. CAD import. The original model, used to model the scene (Chapter 4.3) is imported as a STL file.
5. Alignment between the ideal model (CAD) and the reconstructed model (Mesh). Various alignment strategies can be employed using the software, depending on the function and the part to be

compared. In our case, a pre-alignment of the local best-fit type was performed, having noticed that if the direction of the normal vectors was consistent with the surface and a sufficiently narrow mesh size was used, the algorithm was able to obtain satisfactory results already with pre-alignment. Next, a manual type of alignment was performed, based on the coincidence between CAD and the reconstructed model of the bottom layers of the dovetail. Then using the same type of alignment for all the dovetails, it was possible to graphically obtain the trend of distortions as the parameters considered changed.

The graphical result of the comparison on the blades is shown below. Looking at the blade with a bottom view, it is possible to remark the areas of distortion where thus there is greater lack of material (yellow and red areas).



Figure 6.2: Blades comparison with nominal geometry

Another important factor that transpires from the comparison is the residue trace left by the support on the part (figure 6.3). It is noticeable that in some specimens the trace of the residue left behind is significantly more impactful than in others (in the graph, these are the areas highlighted in blue, with a range of distortion >0.75 mm)

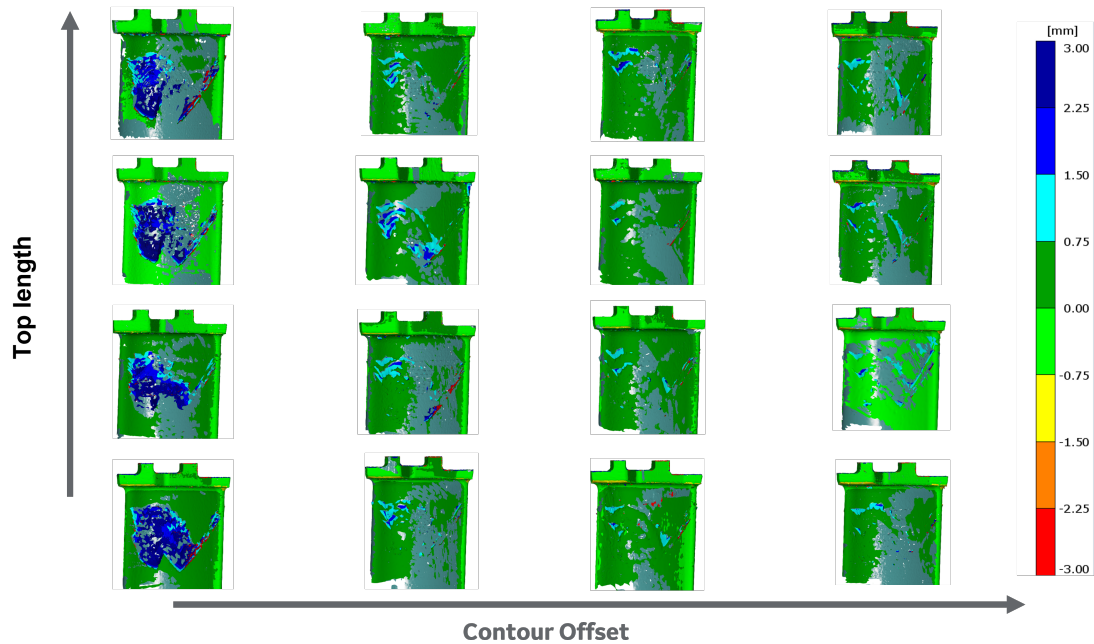


Figure 6.3: Residual traces of supports on the blade

6.2.2 Data processing

Needing the DOE optimization procedure of numerical and quantifiable coefficients (chapter 4.1), the graphical data obtained from the Comparison software were extracted and processed. To do this, deviations from the nominal geometry were exported to an ASCII-format table containing the coordinates of each mesh point and the average distortion of each point. Next, the data were processed using matlab code. Initially, the average distortion of the entire blade was considered.

However, seeing that this data was too much affected by the presence of residue, especially in blades with contour offset 1 supports, it was decided to consider only the negative distortions, i.e., those where compared to the nominal geometry there appears to be a lack of material, thus excluding the positive distortion areas, i.e., those where there was extra material (or residue).

The matlab code used is as follows:

```

somma=0;
n=0;
f_real=fopen('0469T_6.asc', 'r');
C=textscan(f_real, '%s %f %f %f %f %f %f %f %f');
fclose(f_real);
h=C(8);
for i=1:length(h{1,1})
    if h{1,1}(i)>=-3&&h{1,1}(i)<=0
        somma=somma+h{1,1}(i);
        n=n+1;
    end
end
average == somma./n
rateo == n./i
penalized == somma./i

```

Figure 6.4: Matlab script to extract data

It can be seen how the script, considering the entire distortion table, 'filters out' distortions below 3 mm (which do not correspond to physical distortion and result in residual inaccuracy in the mesh) and those greater than zero (for the reason specified above).

The script, then, calculates and returns 3 values for each blade:

- Arithmetic average, which represents the average of the distortions

considered, obtained as:

$$\text{Arithmetic average} = \frac{\text{Sum of distortions}}{\text{Points subject to distortion}}$$

- Ratio, which represents the ratio of distorted area to total area, obtained as:

$$\text{Ratio} = \frac{\text{Points subject to distortion}}{\text{Total points on the surface}}$$

- Penalized average, which represents the product between the two factors:

$$\text{Penalized average} = \text{Arithmetic average} \times \text{ratio}$$

At the level of coherency with the graphical results, the penalized average is the value that appeared most indicative, since it considers within it both the magnitude of distortions and the percentage of distorted area.

By adding the following two lines of code within the script's for loop, moreover, it is possible to obtain a numerical value of the magnitude of the trace of residue left by the support on the part ('res'), considering only positive distortions >0.75 mm.

```
if h{1,1}(i)>=0.75
    res=res+1;
```

The results of the two values for each blade are represented in the table 6.1.

The table shows, respectively:

- The number with which the specimen was marked

- The position of the blade in the build (Chapter 4.3), highlighted with the letter H (High) in the case of blades positioned at the top and L (Low) in those positioned at the bottom.
- The value of Top Length (min a1 , max a4)
- The value of contour offset (min b1, max b4)
- The penalized average
- The amount of residual trace after removal

Standard Order	Position	Top length	Contour offset	Penalized average	Residual
1	L	a4	b1	-0,1401	132445
2	H	a4	b4	-0,2033	12309
3	H	a3	b4	-0,2356	24648
4	L	a4	b2	-0,1435	35765
5	L	a2	b1	-0,1362	51685
6	H	a1	b1	-0,1415	65951
7	H	a4	b3	-0,2271	30859
8	L	a3	b1	-0,1446	101733
9	L	a3	b3	-0,1928	58145
10	H	a2	b4	-0,1959	9816
11	H	a1	b4	-0,1604	8962
12	L	a2	b3	-0,1718	12520
13	L	a3	b2	-0,1562	63145
14	H	a1	b3	-0,155	9117
15	H	a1	b2	-0,1562	14953
16	L	a2	b2	-0,1589	27231

Table 6.1: Data processing results

6.3 Critical analysis of the results

All these results were entered and analyzed in the Minitab program. Minitab is the Statistical Analysis Software for Quality Control, used to analyze the data and improve processes. Minitab, in addition to having all the tools needed to effectively analyze data, helps find meaningful solutions to the most complex business problems most complex, is the standard for Six Sigma and Lean Six Sigma methodologies and is used in various sectors of industry for statistical analysis, cost reduction, increased efficiency, defect reduction and variation control.

The first step was to determine whether the association between the Response and each factor in the model was statistically significant by going to compare the P-Value for each factor with the significance level to assess the null hypothesis. The null hypothesis is that there is no association between the factor and the response. Usually, a level of significance (denoted as α or alpha) of 0.05. A significance level of 0.05 indicates a 5% risk of concluding that an association exists when there is no actual association, thus a low probability of making a mistake by stating that the factor is not statistically significant.

- P-Value $< \alpha$: the association is statistically significant. If the P-value is less than or equal to the significance value, it can be concluded that there is a statistically significant association between the response variable and the factor.
- P-value $> \alpha$: the association is not statistically significant. If the P-value is greater than the significance value, it is not possible to conclude that there is a statistically significant association between the response variable and the factor.

In Figures 6.5, 6.6 and 6.7 is shown what is called the Pareto chart of Effects. This graph is used to compare the relative magnitude and statistical significance of main effects and their interaction.

The graph shows the type of effect as follows:

- If the model does not include an error term, the graph displays the absolute value of the unstandardized effects.
- If the model includes an error term, the graph displays the absolute value of standardized effects.

Minitab plots the effects in the descending order of their absolute values. The line of reference on the graph indicates which effects are significant. By default, minitab uses a significance level of 0.05 to plot the reference line.

The effect of top length, contour offset, and position on the penalized average is investigated in 6.5.

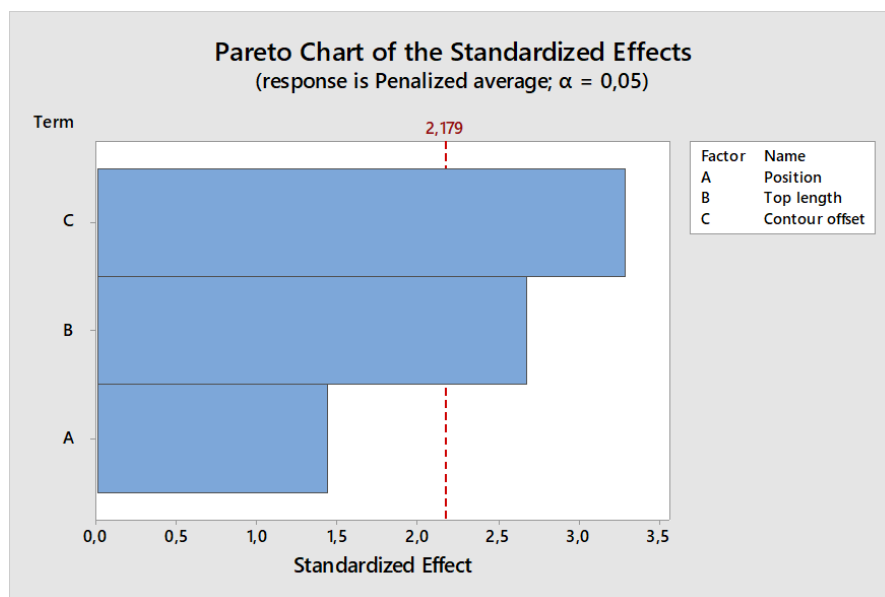


Figure 6.5: Pareto chart on penalized average

It is clear from the graph that only the top length and contour offset affect the change in the penalized mean. The position within the build,

on the contrary, does not affect significantly, so the analysis is repeated considering only the two factors up to order 2 in 6.6. The analysis

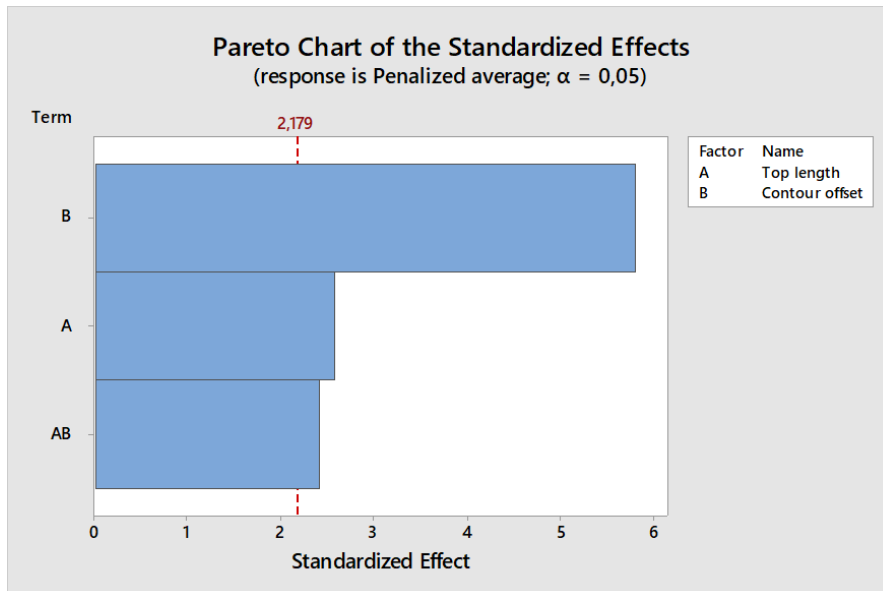


Figure 6.6: Pareto chart on penalized average

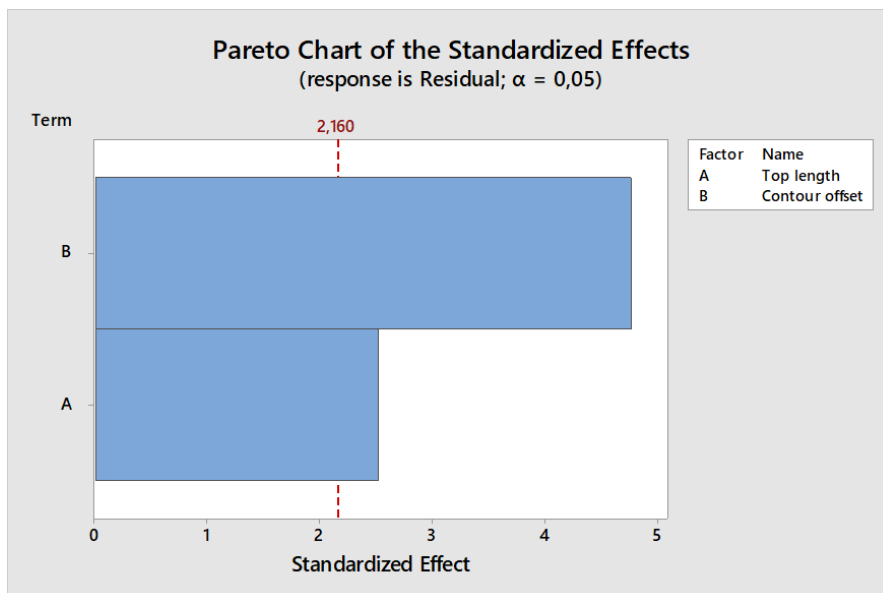


Figure 6.7: Pareto chart on residual

thus shows that contour offset is the variable that most influences the results, while top length and the interaction between the two, while having influence, impact much less significantly.

The procedure was then repeated to study the effects of the geometric shape of the support on the trace of residue left on the blade in 6.7. In this case, however, the top length has a slightly greater influence, although much lower than the contour offset, while the interaction between the two does not significantly affect the result.

In 6.8 and 6.9, the residue plots for the two results considered are shown. The residue plots are automatically generated by minitab and give an idea of how well the mathematical model fits the actual values. The residual represents the normalized value of the difference between the actual value and the calculated value. The lower the residuals, the truer the approximation. The diagram on the upper left represents how the residuals are distributed around the regression line, the further away from the line, the greater the approximation. The two plots on the right, represent the plotting of the residuals as a function of the approximate values and as a function of the standard order for each measurement. The two plots are used to verify that there are no measurements with residuals that are too high relative to the mean, which could then deviate significantly from the trend that is identified. Finally, the bottom right histogram gives an idea of the amount and frequency with which measurement errors recur.

After an iterative process of reconsidering the measurements that were not in line with the trend, it can be seen that all the values are generally coherent and uniformly distributed, which leads to the assertion, with some margin of risk, that the model considered is valid.

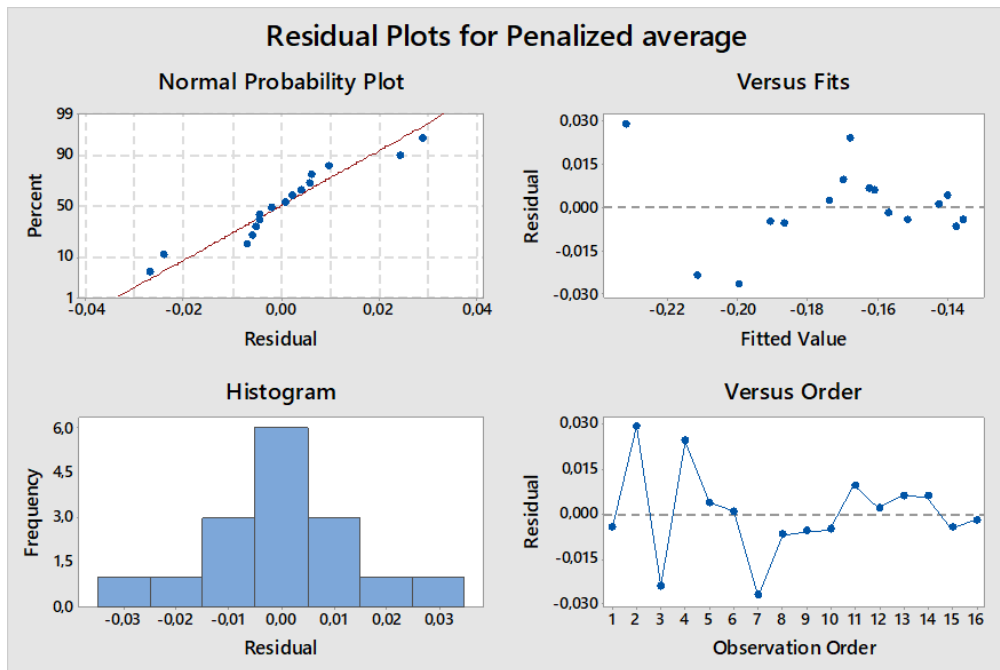


Figure 6.8: Residual plots for penalized average

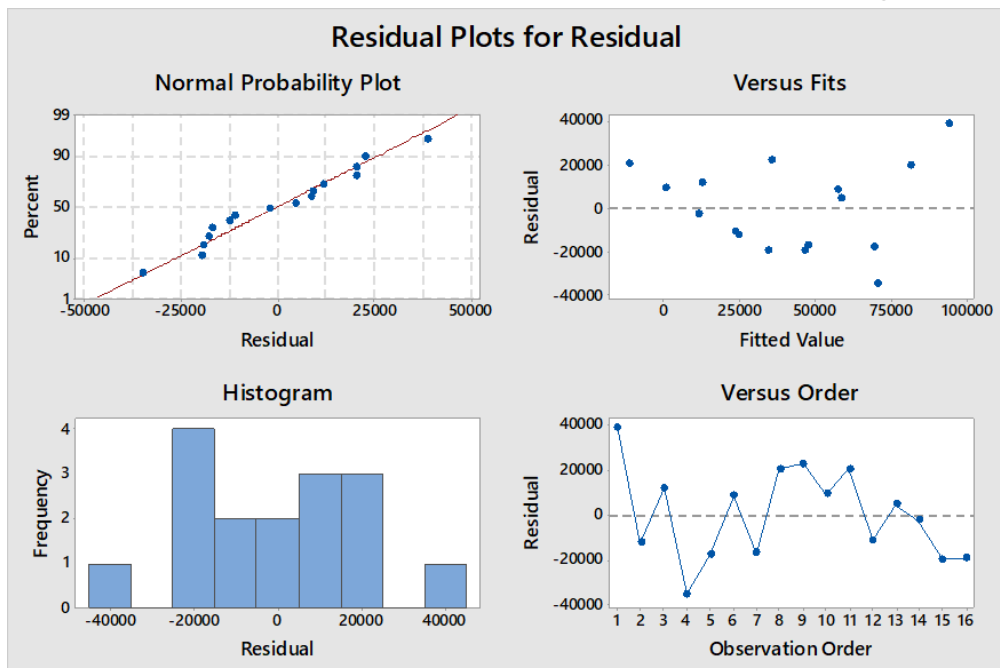


Figure 6.9: Residual plots for trace left by supports

The diagram 6.10 shows the plot of the mathematical model representing the penalized average as a function of top length and contour offset. The areas in dark green are the least distorted areas (> -0.14 mm), those in light green the most distorted areas (< -0.22 mm). The most distorted areas can be identified, based on the boundary conditions considered, with contour offset b4 and top length of a4. In contrast, the least distorted zone results at contour offset b1 and top length a4.

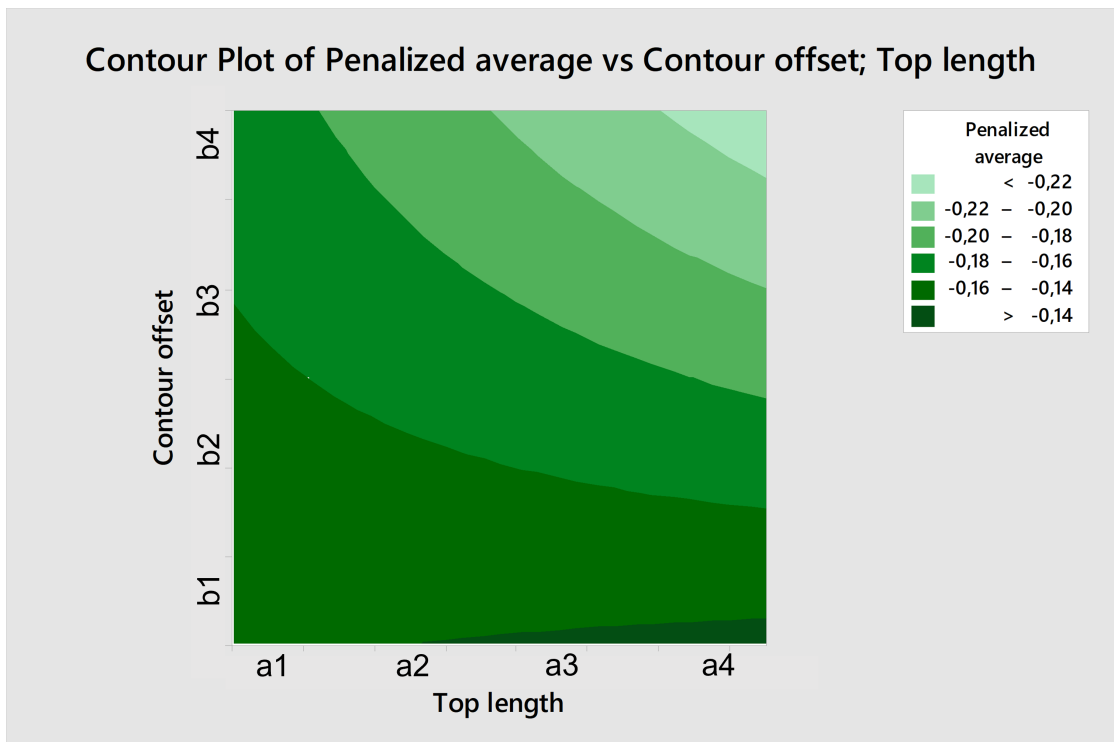


Figure 6.10: Contour plot for penalized average

The model is coherent with the results obtained in chapter 6.2.1, and clearly demonstrates how an increase in contour offset negatively affects blade distortions. In general, therefore, it might be thought that it would be sufficient to use as little contour offset as possible to decrease the total blade distortion, but as specified in chapter 6.2.1 another important factor to take into account in identifying the optimal working

point is the residual trace left by the substrate. Therefore, the contour plot of the residue trace was derived as a function of the contour offset of the top length in 6.11.

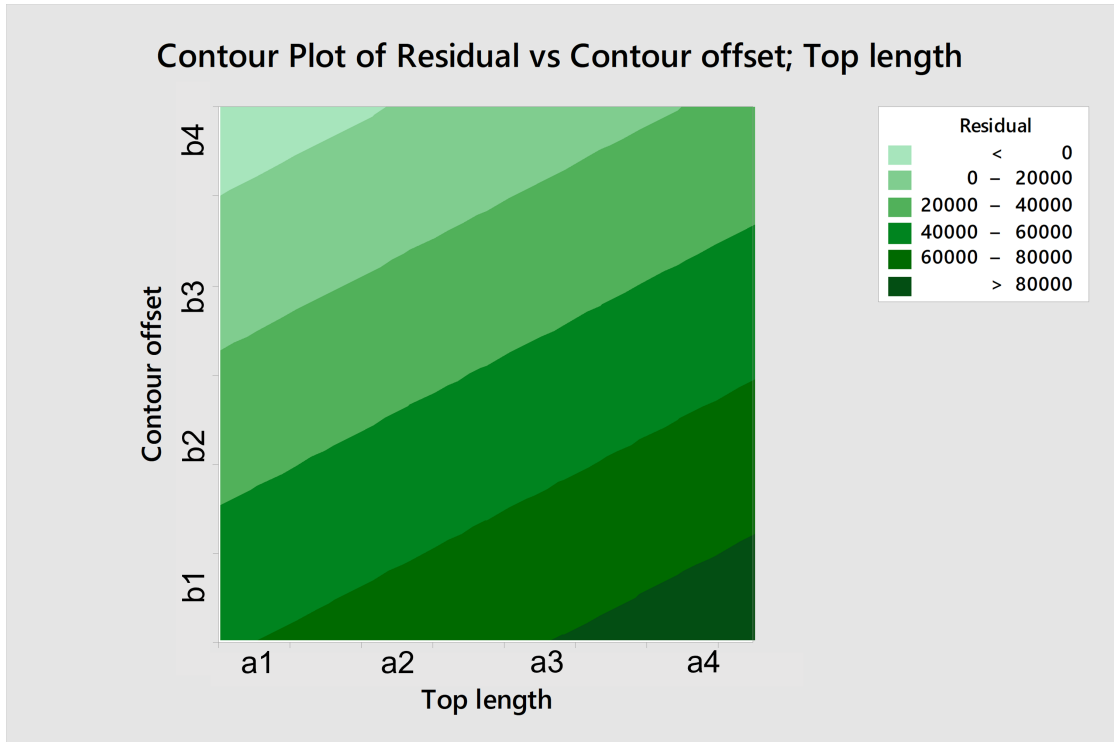


Figure 6.11: Contour plot for penalized average

To combine the two results, via minitab the search for the optimal point through the maxima and minima is possible. Therefore, we proceeded by maximizing the value of penalized average (since it is a negative value) and minimizing the value of the residuals (Figure 6.12), in order to obtain the optimal working point for a support that minimizes distortions but at the same time does not leave too many traces on the part. For the study, equal weight was given to both factors, considering blade distortion and residue trace remaining equally important.

The results of the optimal working point, with the relative predicted values of the average distortion and of the residual trace left, are represented in figure ¹ 6.12.

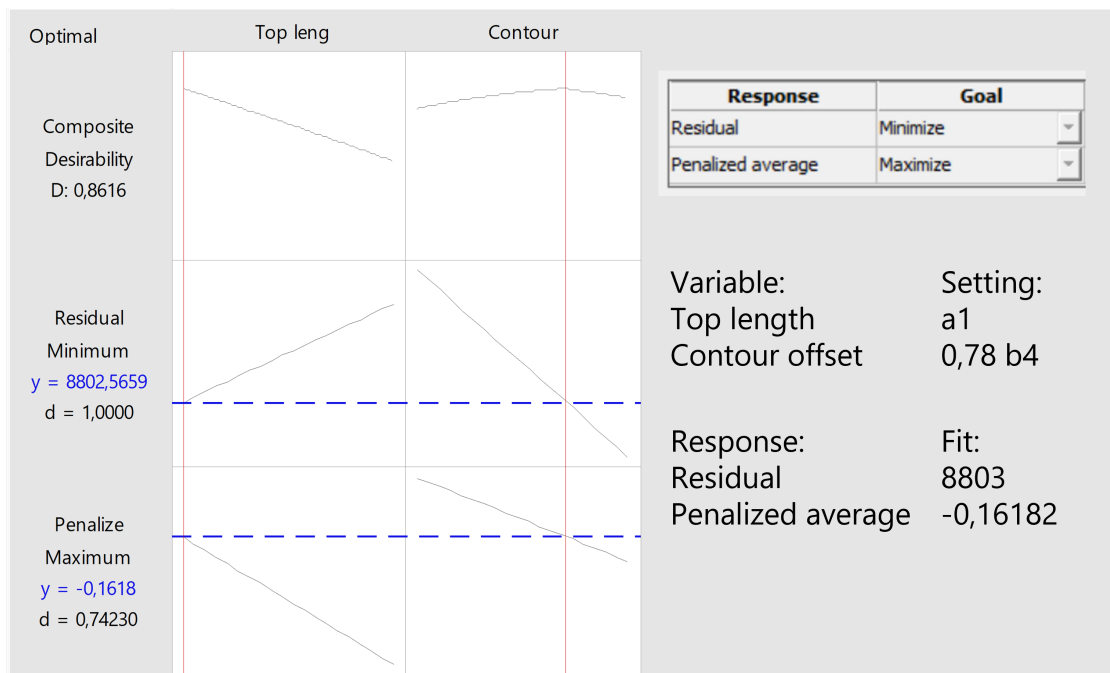


Figure 6.12: DOE optimization setting, search for the optimal values

¹a1=minimum value of the top length, b4=maximum value of the contour offset among those considered as parameters of the DOE

Conclusions

The results obtained from the thesis work lead to the conclusion that there are optimal values for the realization of the supports, and thus in general for the improvement of the process from the perspective of blade distortions and the difficulty of removing the support itself.

Some considerations are necessary for critical analysis of the results. The first is that with the factorial DOE predictive model it is possible to find optimal points but also to give different weight to the functions analyzed. If, for example, it is desired to give more importance to the reduction of distortions on the blade, while still accounting for greater difficulty in removing supports, it is possible to quantify this preference by assigning a penalty factor to the second output. This could be the case, for example, with very stringent quality controls, which have not been taken into account for the purposes of this work, but which could lead to a preference for a part that is more dimensionally accurate and more expensive to refine in the post-processing phase.

Another note that needs to be made is that only the geometric parameters of the substrate were considered within this study, but neither the process parameters, summarized in chapter 2.1.4, nor any manufacturing defects (chapter 2.2.1) were examined, except through thermal analysis. A future extension of this study, therefore, might involve adding process parameters such as electron beam intensity or thermal

energy delivered during preheating step 2 (chapter 2.1.3), or even consider additional geometric parameters of contour-type supports, such as tooth-to-tooth spacing or fin thickness, which were established at the beginning of the study as less relevant, but which might also have a minimal influence on the effects considered.

Inside the paper, the exact values of the currently used parameters, and of the derived optimal ones, have not been published, as they are key-features of the production and intellectual property of Avio Aero s.r.l.

Appendix A

EBM machinery

	Main features	Datasheet	Feedstock Materials
Arcam EBM Q20plus 	<p>Specifically designed for cost-efficient production of aerospace components, such as turbine blades, structural airframe components and much more.</p>	<p>BUILD VOLUME: 350 x 380 (∅/H)</p> <p>ELECTRON BEAM POWER: 3kW</p>	<p>Arcam EBM Ti6Al4V Grade 5, P-Material</p> <p>Arcam EBM Ti6Al4V Grade 23, P-Material</p>
Arcam EBM A2X 	<p>Low operational cost, low cost of consumables, efficient reuse of powder and low powder cost.</p> <p>For academia and research institutes, the build chamber of the A2X is specifically designed to withstand extremely high process temperatures over 1,100° C.</p>	<p>BUILD VOLUME: 200 x 200 x 380 mm (LxWxH)</p> <p>ELECTRON BEAM POWER: 3kW</p>	<p>Arcam EBM Ti6Al4V Grade 5, P-Material</p> <p>Arcam EBM Ti6Al4V Grade 23, P-Material</p> <p>Arcam EBM Nickel alloy 718, D-Material</p> <p>Arcam EBM TiAl, D-Material</p>
Arcam EBM Spectra H 	<p>The Spectra H has the capability to produce parts at temperatures exceeding 1,000 °C. The high-heat capability enables users to incorporate new alloys, including high-temperature, crack-prone materials.</p>	<p>BUILD VOLUME: 250 x 430 mm (∅/H)</p> <p>ELECTRON BEAM POWER: 6kW</p>	<p>Arcam EBM Ti6Al4V Grade 5</p> <p>Arcam EBM TiAl,</p> <p>Arcam EBM Nickel alloy 718,</p> <p>Arcam EBM Highly Alloyed Tool Steel</p>

Bibliography

- [1] Tanisha Pereira, John V Kennedy, and Johan Potgieter. «A comparison of traditional manufacturing vs additive manufacturing, the best method for the job». In: *Procedia Manufacturing* 30 (2019). Digital Manufacturing Transforming Industry Towards Sustainable Growth, pp. 11–18. ISSN: 2351-9789. DOI: <https://doi.org/10.1016/j.promfg.2019.02.003>. URL: <https://www.sciencedirect.com/science/article/pii/S2351978919300332> (cit. on pp. 3, 11).
- [2] J.-P. Kruth, M.C. Leu, and T. Nakagawa. «Progress in Additive Manufacturing and Rapid Prototyping». In: *CIRP Annals* 47.2 (1998), pp. 525–540. ISSN: 0007-8506. DOI: [https://doi.org/10.1016/S0007-8506\(07\)63240-5](https://doi.org/10.1016/S0007-8506(07)63240-5). URL: <https://www.sciencedirect.com/science/article/pii/S0007850607632405> (cit. on p. 3).
- [3] Mariano Jiménez, Luis Romero, Iris A. Domínguez, María del Mar Espinosa, and Manuel Domínguez. «Additive Manufacturing Technologies: An Overview about 3D Printing Methods and Future Prospects». In: *Complexity* 2019 (Feb. 2019), p. 9656938. ISSN: 1076-2787. DOI: [10.1155/2019/9656938](https://doi.org/10.1155/2019/9656938). URL: <https://doi.org/10.1155/2019/9656938> (cit. on p. 4).
- [4] K. Reddy and Solomon Dufera. «ADDITIVE MANUFACTURING TECHNOLOGIES». In: (July 2019) (cit. on p. 4).

- [5] Carlos M. González. «Infographic:3D Printing». In: (Gen 2020). URL: <https://www.asme.org/topics-resources/content/infographic-the-history-of-3d-printing> (cit. on pp. 5, 6).
- [6] Education Department at the Museum of Arts, Centre for Fine Print Research Design with special assistance from Stephan Hoskins and Materialise. Vanessa Palsenbarg. «3D PRINTING TIME-LINE». In: (). URL: <https://madmuseum.org/sites/default/files/static/ed/3D%20Printed%20Timeline%20Resource.pdf> (cit. on pp. 5–7, 18).
- [7] Matthias Schmidt-Lehr Dr. Maximilian Munsch and Dr. Eric Wycisk. «AMPOWER Report on Additive Manufacturing». In: (Mar. 2021). URL: <https://additive-manufacturing-report.com/> (cit. on p. 7).
- [8] MARK COTTELEER and JIM JOYCE. «3DOppportunity Additive manufacturing paths to performance, innovation, and growth». In: (June 2014) (cit. on p. 8).
- [9] Babak Mohajeri, Jürgen Poesche, Ilkka Kauranen, and Timo Nyberg. «Shift to social manufacturing: Applications of additive manufacturing for consumer products». In: *2016 IEEE International Conference on Service Operations and Logistics, and Informatics (SOLI)*. 2016, pp. 1–6. DOI: 10.1109/SOLI.2016.7551652 (cit. on p. 8).
- [10] Terry Wohlers and Tim Gornet. «3History of additive manufacturing, Wohlers Report». In: (2018). URL: <https://www.wohlersassociates.com/history2016.pdf> (cit. on pp. 8, 10).
- [11] Thierry Rayna and Ludmila Striukova. «From rapid prototyping to home fabrication: How 3D printing is changing business model innovation». In: *Technological Forecasting and Social Change* 102 (2016), pp. 214–224. ISSN: 0040-1625. DOI: <https://doi.org/10.1016/j.techfore.2016.05.010>

- org/10.1016/j.techfore.2015.07.023. URL: <https://www.sciencedirect.com/science/article/pii/S0040162515002425> (cit. on p. 8).
- [12] I. Gibson, D. Rosen, and B. Stucker. *Additive Manufacturing Technologies: 3D Printing, Rapid Prototyping, and Direct Digital Manufacturing*. Springer New York, 2014. ISBN: 9781493921133. URL: <https://books.google.it/books?id=OPGbBQAAQBAJ> (cit. on p. 9).
- [13] Joel C. Najmon, Sajjad Raeisi, and Andres Tovar. «2 - Review of additive manufacturing technologies and applications in the aerospace industry». In: *Additive Manufacturing for the Aerospace Industry*. Ed. by Francis Froes and Rodney Boyer. Elsevier, 2019, pp. 7–31. ISBN: 978-0-12-814062-8. DOI: <https://doi.org/10.1016/B978-0-12-814062-8.00002-9>. URL: <https://www.sciencedirect.com/science/article/pii/B9780128140628000029> (cit. on p. 9).
- [14] Tamburrino Francesco, Valeria Perrotta, Raffaella Aversa, and Antonio Apicella. «Additive technology and design process: an innovative tool to drive and assist product development». In: June 2015 (cit. on p. 10).
- [15] Ugur M. Dilberoglu, Bahar Gharehpapagh, Ulas Yaman, and Melik Dolen. «The Role of Additive Manufacturing in the Era of Industry 4.0». In: *Procedia Manufacturing* 11 (2017). 27th International Conference on Flexible Automation and Intelligent Manufacturing, FAIM2017, 27-30 June 2017, Modena, Italy, pp. 545–554. ISSN: 2351-9789. DOI: <https://doi.org/10.1016/j.promfg.2017.07.148>. URL: <https://www.sciencedirect.com/science/article/pii/S2351978917303529> (cit. on p. 14).
- [16] Dr Harald Proff and Andreas Staffen. «Challenges of additive manufacturing, why company don't use additive manufacturing in production». In: *DELOITTE* (2019). URL: <https://www2.>

- `deloitte.com/content/dam/Deloitte/de/Documents/operations/Deloitte_Challenges_of_Additive_Manufacturing.pdf` (cit. on p. 14).
- [17] Nannan Guo and Ming Leu. «Additive manufacturing: Technology, applications and research needs». In: *Frontiers of Mechanical Engineering* 8 (Sept. 2013). DOI: [10.1007/s11465-013-0248-8](https://doi.org/10.1007/s11465-013-0248-8) (cit. on pp. 15, 31).
- [18] S.J. Kalita. «13 - Rapid prototyping in biomedical engineering: structural intricacies of biological materials». In: *Biointegration of Medical Implant Materials*. Ed. by Chandra P. Sharma. Woodhead Publishing Series in Biomaterials. Woodhead Publishing, 2010, pp. 349–397. ISBN: 978-1-84569-509-5. DOI: <https://doi.org/10.1533/9781845699802.3.349>. URL: <https://www.sciencedirect.com/science/article/pii/B9781845695095500136> (cit. on p. 16).
- [19] R. Singh, S. Singh, and M.S.J. Hashmi. «Implant Materials and Their Processing Technologies». In: *Reference Module in Materials Science and Materials Engineering*. Elsevier, 2016. ISBN: 978-0-12-803581-8. DOI: <https://doi.org/10.1016/B978-0-12-803581-8.04156-4>. URL: <https://www.sciencedirect.com/science/article/pii/B9780128035818041564> (cit. on pp. 16, 18).
- [20] *EBM machines solutions*. <https://www.ge.com/additive/additive-manufacturing/machines/ebm-machines>. Accessed: 2022-07 (cit. on pp. 18, 27).
- [21] Manuela Galati, Luca Iuliano, Alessandro Salmi, and Eleonora Atzeni. «Modelling energy source and powder properties for the development of a thermal FE model of the EBM additive manufacturing process». In: *Addit. Manuf.* 14 (Mar. 2017), pp. 49–59 (cit. on pp. 20, 54).

- [22] Balaji Soundararajan, Daniele Sofia, Diego Barletta, and Massimo Poletto. «Review on modeling techniques for powder bed fusion processes based on physical principles». In: *Additive Manufacturing* 47 (2021), p. 102336. ISSN: 2214-8604. DOI: <https://doi.org/10.1016/j.addma.2021.102336>. URL: <https://www.sciencedirect.com/science/article/pii/S2214860421004942> (cit. on p. 22).
- [23] Manuela Galati. «Chapter 8 - Electron beam melting process: a general overview». In: *Additive Manufacturing*. Ed. by Juan Pou, Antonio Riveiro, and J. Paulo Davim. Handbooks in Advanced Manufacturing. Elsevier, 2021, pp. 277–301. ISBN: 978-0-12-818411-0. DOI: <https://doi.org/10.1016/B978-0-12-818411-0.00014-8>. URL: <https://www.sciencedirect.com/science/article/pii/B9780128184110000148> (cit. on p. 24).
- [24] Babar Saleem. «Characterization of the EBM Additive Manufacturing Process Parameters using Artificial Neural Networks». In: *webthesis polito* (). URL: <https://webthesis.biblio.polito.it/16684/1/tesi.pdf> (cit. on p. 25).
- [25] Chee Kai Chua, Chee How Wong, and Wai Yee Yeong. «Chapter One - Introduction to 3D Printing or Additive Manufacturing». In: *Standards, Quality Control, and Measurement Sciences in 3D Printing and Additive Manufacturing*. Ed. by Chee Kai Chua, Chee How Wong, and Wai Yee Yeong. Academic Press, 2017, pp. 1–29. ISBN: 978-0-12-813489-4. DOI: <https://doi.org/10.1016/B978-0-12-813489-4.00001-5>. URL: <https://www.sciencedirect.com/science/article/pii/B9780128134894000015> (cit. on p. 26).
- [26] *Gas Atomization*. <https://www.beyonddiscovery.org/powder-metallurgy/gas-atomization.html#:~:text=Gas%20atomization%20is%20the%20process,water%20atomization%20in%20many%20respects..> Accessed: 04 Jul 2022 (cit. on p. 27).

- [27] *Introduction to the SLM process*. <https://www.birmingham.ac.uk/research/activity/metallurgy-materials/amplab/projects/slm.aspx>. Accessed: 06 Jul 2022 (cit. on p. 28).
- [28] Raya Mertens, Sasan Dadbakhsh, Jan Humbeeck, and Jean-Pierre Kruth. «Application of base plate preheating during selective laser melting». In: *Procedia CIRP* 74 (Jan. 2018), pp. 5–11. DOI: 10.1016/j.procir.2018.08.002 (cit. on p. 29).
- [29] *AM process in general*. https://formnext.mesago.com/frankfurt/en/themes-events/am-field-guide/process_in_general.html. Accessed: 2022-06 (cit. on p. 33).
- [30] Mary Kathryn Thompson et al. «Design for Additive Manufacturing: Trends, opportunities, considerations, and constraints». In: *CIRP Annals* 65.2 (2016), pp. 737–760. ISSN: 0007-8506. DOI: <https://doi.org/10.1016/j.cirp.2016.05.004>. URL: <https://www.sciencedirect.com/science/article/pii/S0007850616301913> (cit. on p. 34).
- [31] *STL (STereoLithography) File Format Family*. <https://www.loc.gov/preservation/digital/formats/fdd/fdd000504.shtml>. Accessed: 09/11/2020 (cit. on p. 34).
- [32] *ASCII stereolithography files*. <https://people.math.sc.edu/Burkardt/data/stla/stla.html>. Last revised on 10 July 2014. (cit. on p. 35).
- [33] Omar Mohamed. «Analytical Modeling and Experimental Investigation of Product Quality and Mechanical Properties in FDM Additive Manufacturing». PhD thesis. Sept. 2019. DOI: 10.13140/RG.2.2.28847.48807 (cit. on p. 36).
- [34] Adam Ellis, Ryan Brown, and Neil Hopkinson. «The effect of build orientation and surface modification on mechanical properties of high speed sintered parts». In: *Surface Topography: Metrology and Properties* 3 (Sept. 2015), p. 034005. DOI: 10.1088/2051-672X/3/3/034005 (cit. on p. 38).

- [35] Torbjørn Langedahl Leirimo, Oleksandr Semeniuta, and Kristian Martinsen. «Tolerancing from STL data: A Legacy Challenge». In: *Procedia CIRP* 92 (2020). 16th CIRP Conference on Computer Aided Tolerancing (CIRP CAT 2020), pp. 218–223. ISSN: 2212-8271. DOI: <https://doi.org/10.1016/j.procir.2020.05.180>. URL: <https://www.sciencedirect.com/science/article/pii/S221282712030946X> (cit. on p. 39).
- [36] Nan Luo and Quan Wang. «Fast slicing orientation determining and optimizing algorithm for least volumetric error in rapid prototyping». In: *The International Journal of Advanced Manufacturing Technology* 83 (Aug. 2015). DOI: [10.1007/s00170-015-7571-7](https://doi.org/10.1007/s00170-015-7571-7) (cit. on p. 41).
- [37] Mahmood, Chioibas Diana, Asif Rehman, Sabin Mihai, and Andrei Popescu. «Post-Processing Techniques to Enhance the Quality of Metallic Parts Produced by Additive Manufacturing». In: *Metals - Open Access Metallurgy Journal* 12 (Jan. 2022), p. 77. DOI: [10.3390/met12010077](https://doi.org/10.3390/met12010077) (cit. on p. 42).
- [38] Martín Tanco, Elisabeth Viles, Laura Ilzarbe, and M.J. Alvarez. «Implementation of Design of Experiments projects in industry». In: *Applied Stochastic Models in Business and Industry* 25 (July 2009), pp. 478–505. DOI: [10.1002/asmb.779](https://doi.org/10.1002/asmb.779) (cit. on pp. 43, 44).
- [39] Seu Gianluca. «Analisi dei parametri influenti su comportamento elastodinamico di tendicinghia». PhD thesis. Dec. 2018 (cit. on p. 43).
- [40] Manuela Galati, Oscar Di Mauro, and Luca Iuliano. «Finite Element Simulation of Multilayer Electron Beam Melting for the Improvement of Build Quality». In: *Crystals* 10 (June 2020), p. 532. DOI: [10.3390/cryst10060532](https://doi.org/10.3390/cryst10060532) (cit. on pp. 51, 56).

BIBLIOGRAPHY

- [41] Manuela Galati and Luca Iuliano. «A literature review of powder-based electron beam melting focusing on numerical simulations». In: *Additive Manufacturing* 19 (Nov. 2017). DOI: 10.1016/j.addma.2017.11.001 (cit. on pp. 52, 53, 56, 57).
- [42] B. Lofving S. Johansson and A. Snis. «A new heat model for improved control of build temperature». In: *Arcam, GE* () (cit. on p. 58).